Reply to reviewer 1

(our response **in bold font**)

We thank the reviewer for the helpful comments. We totally agree with his concerns about degrees of freedom in the data set and had this already included in the previous version of the manuscript, however we missed to describe it in detail in the text. For trends computations the effective degrees of freedom of N*=N/T was already used in our Matlab routine for trend computation in the submitted version. We edited the revised text accordingly and now describe in detail how the degrees of freedom are derived. The autocorrelation of each time series is used to determine the statistical independence of measurements in successive years and the half folding width is used to calculate the degrees of freedom of the time series, respectively to the distribution of data points. The routine used for trend computation is included at the end of this text. For the trend computation and autocorrelation we describe now in the text: 'For the trend computation, successive years of the time series are not necessarily statistically independent of each other. Therefore we determined the effective number of degrees of freedom for the computation of the confidence interval. For each time series the lag dependent temporal half folding range of the autocorrelation function was used to compute the degrees of freedom. The length of the time series was divided by the length of the time derived from the autocorrelation function, giving a statistical measure of the degrees of freedom for each analysed time series independently. The correlation coefficient and significance between the oxygen time series and the PDO or NPGO were computed for all years available, using a chi-squared test with the degrees of freedom as computed above.'.

GENERAL ASSESSMENT

Dr Lothar Stramma and coauthors compiled a mostly public dataset of oxygen, nitrate, silicate and phosphate observations from eight areas of the Pacific Ocean. Using those data, they calculated long-term trends over the entire length of the time series. They also calculated trends over the 1950 to 1976 negative phase of the Pacific Decadal Oscillation (PDO), and after 1976 for the positive phase of the PDO. They showed that in some cases, trend estimates were very different depending on sign of PDO phase.

In addition, they calculated lagged correlation coefficients between oxygen, nutrient and temperature time series from their eight areas with the PDO and with the North Pacific Gyre Oscillation (NPGO) climate indices. They also briefly examined how three other modes of climate variability (ENSO, STC, NPI) may or may not affect the time series in the same eight areas.

This is a worthwhile study. It is important that we better understand “The influence of decadal oscillations on the oxygen and nutrient trends in the Pacific Ocean”. But there is a big caveat: the word DECADAL in the paper’s title aptly captures the idea that successive years are not statistically independent of each other. For instance, when a given year is above normal for the PDO, the odds of having a below normal value of the PDO the following year is actually lower than 0.5; the dice are rigged. Several consecutive years with above normal values tend to be lumped together, and likewise for below normal values. From the point of view of statistical analysis, this implies the assumption that successive annual values in the oxygen, nutrients and temperature time series are independent of each other is not valid. Consequently, the effective number of degrees of freedom N* will often be much less than the number of years N, so that 95% confidence intervals will be broader than those assumed in the submitted paper, and some trends (Tables 1 and S1) that are considered statistically different from zero at the 0.05 level in the paper probably are not.

Given that trend estimation and determination of their confidence intervals is a key component of this paper, I consider a major revision of the paper will be required to take serial correlation (autocorrelation) of time series into account.

As explained above we had already used the effective degrees of freedom and mention it now more clearly in the text and we changed the serial correlation, as described also below. For the area P e.g. the degrees of freedom for oxygen trends were 13.8 for 23 available years for the period 1954- 1976, 33.9 for 40 years 1977 to 2017 and 50.8 for 63 years 1954-2017. The degrees of

freedom depend strongly on the data set and time series analyzed. The method is now described in the text.

MAJOR COMMENTS

The “Data Processing” section of the paper is extremely succinct about the methods used for the computation of trends (p. 9, lines 3-6), the computation of correlation coefficients (p.10, lines 1-3) and their confidence intervals and significance levels. Upon examining the trends and correlation coefficients considered statistically different from zero in the text and Tables, I came to the conclusion that the authors used statistical methods that assume iid (independent identically distributed) variables. This is a major issue, because neglecting autocorrelation (aka serial correlation) in the time series can invalidate the levels of statistical significance and confidence intervals that are found throughout the text and in the Tables of results (von Storch and Zwiers 1999).

The Data processing explanation for the trend was extended with the information on the use of effective number of degrees of freedom for the computation of the confidence intervals, as well as the p-values for the correlations.

The authors did not perform a runs test for randomness to verify the underlying assumption that successive yearly values in their time series are independent of each other. Using the links provided by the authors, I downloaded yearly values (1950- 2017) for the PDO index, and I downloaded monthly values for the NPGO index from which I then computed yearly averaged values from 1950 to 2017. Using a runs test for randomness on the PDO time series, the null hypothesis that the yearly values of the PDO index come in random order is rejected (p = 2.5e-08). Likewise, using a runs test for randomness on the NPGO time series, the null hypothesis that the yearly values of the NPGO index come in random order is also rejected (p = 0.0053).

Given this, it appears that neglecting to take into account autocorrelation in the statistical analyses of trends (for individual time series) and correlation coefficients (for paired time series) is an important flaw in a paper whose intent is to focus on the influence of decadal climate variability on yearly oxygen and nutrient time series. But luckily this flaw can be fixed, as methods that account for autocorrelation by adjusting the number of effective degrees of freedom do exist. For trends calculations, Thomson and Emery (2014) propose dividing the length of the time series N by an integral time scale T in order to obtain an effective number of degrees of freedom N* = N/T. Using their method for estimating an integral time scale by including lags of up to plus or minus 10 years for example, I obtained an integral time scale for the PDO time series of 2.8 years. This implies that on average, we get independent values of the PDO index every 3 years or so.

Autocorrelation of time series is not only a problem for trends estimation. It also affects confidence intervals for correlation coefficients of paired time series. When we have N pairs of (x,y) values, the effective number of degrees of freedom N* is not equal to N-2 as assumed by the authors, but is generally smaller. A resampling scheme that reduces the impact of serial correlation on inferences made about the correlation coefficient is described by Ebisuzaki (1997), who also provides a review of other techniques that correct for autocorrelation in the estimation of confidence intervals for correlation coefficients.

As mentioned above we made the trend computations using the effective degrees of freedom N*=N/T, however it was not described in the text and now a statement is added in the revised version. Successive years are not assumed to be statistically independent except the autocorrelation function does indicate so. Never the less, with short and non continuous time series, methods and statistical analysis is limited to a degree.

MINOR COMMENTS

1. p.6, line3-4; and 5 CONSECUTIVE months of at least -0.5_C are defined as La Niña Events

‘CONSECUTIVE’ added

2. p.6, line 16; the discarding OF already sparse data

‘OF’ added

3. p.8, lines 14-16; the squares and circles are difficult to tell apart from each other, possibly because they are too small. Using circles and triangles (instead of squares) might provide a better visual contrast. This comment about squares and circles also applies to figures 3, 4, 5, 7, S2, S3, S4, S5.

Triangles were also difficult to separate from circles and did not cover the entire crosses, therefore me modified all figures by showing the circles in magenta and the squares in blue.

4. p.9, line 22; Do the spatial scales of 50 m and 100 m apply to both the horizontal and vertical directions? If not, the word "spatial" should be replaced with either vertical or horizontal.

"spatial" was replaced by "vertical"

5. p.15, line 20; replace thEn with thAn

thEn replaced by thAn

6. p.17, lines 25-27; A correlation is significant at r = -0.27, and another is not significant at r = 0.25. But one suspects that the p-value associated with r = -0.27 is barely below 0.05 whereas the p-value associated with r = 0.25 is barely above 0.05. A growing number of scientists insist that giving the actual p-values in the text and in tables is actually preferable to the dichotomy of dividing them in two categories: significant or not significant. See McShane et al. (2019) and other papers in a special issue of The American Statistician entirely dedicated to "A world beyond p < 0.05". I would love to see more p-values throughout the text and tables of this paper.

The p-values were added to table 2 and statistical significance based on p-values were removed in the text. The references to the papers by McShane et al. 2019 and Amrhein et al. 2019 are referenced to explain why no significance statement is given.

7. p.29, line 4; "Trends not within the 95% confidence interval are shown in italics" probably does not convey the intended message. Based on the table, I am guessing the intent was to write "Trends whose 95% confidence interval includes zero are shown in italics", or something like that.

As proposed we modified the text in Table 1 and Table S1 to "Trends whose 95% confidence interval includes zero are shown in italics"

8. p.31; Table 2; Add 2 columns with p-values, one for the PDO-correlation, and the other for the NPGO-correlation. The effective number of degrees of freedom N*-2 (not N-2) should be used to estimate p-values.

p-values are now added in table 2.

9. Figure 6; add the label “Lag (years)” to the the x-axis of the left and right panels.

“Lag (year)”was added to both frames in Figure 6.

REFERENCES

Ebisuzaki, W., 1997. A method to estimate the statistical significance of a correlation when the data are serially correlated. Journal of Climate, 10(9), 2147-2153.

McShane, B.B., Gal, D., Gelman, A., Robert, C. & Tackett, J.L., 2019. Abandon Statistical Significance. The American Statistician, 73:sup1, 235-245.

Von Storch, H. & Zwiers, F. W., 1999. Statistical analysis in climate research. Cambridge University Press, 494p.

Thomson, R. E., & Emery, W. J., 2014. Data analysis methods in physical oceanography. Newnes, 716p. See section 3.15.2 on “Trend estimates and the integral timescale”.

The reference McShane et al. 2019 and in addition Amrhein et al. 2019 were included.

Matlab routine used for trend computations:

```
% version for oxygen in micromoles/kg
q=load('wiwi2.dat');
t=q(:,1)'; tm=mean(t); t=t-tm;
y=q(:,2)';
E=[t',ones(size(t))'];
covmat=inv(E'*E);
model=covmat*E'*y';
res=E*model-y';
c_res=xcorr(res,'coeff');
ii=ceil(length(c_res)/2):length(c_res);
tscale=2*max(cumtrapz([0:length(ii)-1],c_res(ii)));
```

```
% next line introduced 3 May 2010
tscale = max([tscale,1]);
degfree=(size(E,1)/tscale-size(E,2));
chisqr=sum(res.^2)/degfree;
model_err=sqrt(diag(covmat)*chisqr);
y_model=t*model(1)+model(2);
y_model_err_95=student(degfree)*sqrt(model_err(2)^2+(t*model_err(1)).^2);
plot(t+tm,y,'r.',t+tm,y_model,'b-',t+tm,y_model+y_model_err_95,'m--',t+tm,y_model-
y_model_err_95,'m--')
disp(['The linear trend is ',num2str(model(1),3),' micromoles/kg/yr'])
disp(['The formal 95% confidence intervals for that trend are +/-
',num2str(model_err(1)*student(degfree),3),' micromoles/kg/yr'])
% next line introduced 30 April 2010
dof=(size(E,1)-size(E,2))/tscale
```

Reply to reviewer 2

(our response **in bold font**)

We thank the reviewer for the helpful comments.

First, I am a physical oceanographer with insufficient knowledge on biogeochemistry, so I am not confident if I can properly judge this manuscript.

Biogeochemical measurements are definitely more difficult than physical ones, and the time series in each region shown in the manuscript must be valuable themselves. Nevertheless, Secs. 3.2 through 3.4, which should be the main result of this manuscript (inferred from its title), shows rough analyses with little plausible physical mechanisms.

Right, biogeochemical measurements are more difficult than physical ones, and also less biogeochemical measurements are available. Therefore, very few observations of long-term nutrient changes exist, which was the motivation for this manuscript. Changes are observed to be related to long-term trends and in addition to different climate signals related physical mechanisms but also to local biological conditions. The inclusion of the proposed 137°E section helped to put the observations better into the context of the PDO.

My biggest question is, in Sec. 3.2, why the authors show a linear trend for the whole period after 1976 (Fig. 3 and other figures) although they state that "the period 1998 to 2013 is dominated by negative seasonal mean PDO indices and is typically considered as a cool (negative) PDO phase" (Page 5, Line 3-5). If they are to see the relation between the biogeochemical variability and PDO, don't they need to calculate the trend for each of three periods (-1976, 1977-1998, and 1998-2013)?

As the data base for nutrient measurements is small compared to oxygen and temperature measurements especially in regions with no continuous measurements, we think that another subdivision would stress the data set too much. As written in the text in the areas E and D the nutrient data base is so low, that we even did not show the nutrient trend figures. For the area 2-5°S 84-87°W (Fig. 4) only two measurements are available for the period 1998 to 2013 and in the Peru region (now Suppl. Fig. S6) there is a data gap between 1985 and 2008. We added in the concluding results: "…the results might have larger uncertainties for the areas with low data coverage and the combination of the warm and cold PDO periods after 1976". While the reviewer is correct that the overall trend here is not that meaningful with the underlying strong variability, never-the-less it is presented for constancy with the other areas.

Furthermore, although “it is expected that during cold PDO phases the oxygen will decrease and the nutrients increase in the eastern equatorial and tropical Pacific, while during warm PDO periods the oxygen should increase and the nutrients decrease” (Page 13, Line 11-13), the observed trends in areas E, D, G were opposite. So, what is the mechanism? As a non-expert in this field, I feel a bit hard to find what the new findings of this manuscript are.

The expectation mentioned on page 13 lines 11-13 is based on a possible PDO influence on the thermocline depth in a model by Deutsch et al., 2011 and a general Pacific Ocean description by Chavez et al., 2003. The new finding is that in real measurements these changes can’t be always seen, which means that other mechanisms are influencing the oxygen and nutrient distribution and local changes have to be validated by measurements.

Other comments:

Sec. 2.1: Subtropical cell (STC) is an ocean circulation component and is not temporospatial variability. Therefore, I feel odd to see that STC is aligned with climate variability such as PDO, NPGO, and ENSO as a controlling factor.

As mentioned in the text, according to Hong et al., 2014 the STC is strongly associated with the PDO. However, as model simulations by Duteil et al. 2014 described changes in oxygen and phosphate transport, we wanted to check this with measurements.
Still, the reviewer is correct, STCs can be modified and rely on the PDO, we modified the manuscript and now excluded STCs from our analysis, to focus more on the trends with significant impact.

Sec. 2.2: The authors’ data do not cover the western part of the North Pacific Ocean (Fig. 2). Why not the authors use the 137E repeat hydrographic section maintained by the Japan Meteorological Agency since 1967 although one of them belongs to the agency? With high temporal resolution and large spatial (meridional) extent, the section is expected greatly to fill the data gaps.

Now an area of the 137°E section is included to better cover also the Northwestern Pacific. The added area helped a lot to describe the results of the different areas in this manuscript in relation to the PDO.

Page 14, Line 19-20, “probably caused by water masses propagating by 5 to 15 years from Oyashio region into this part of the North Pacific”: why do the authors consider horizontal advection for the area P only?

This water would propagate further southeastward with the subtropical gyre towards the CalCOFIc region. The other regions in the North Pacific show a larger correlation with the PDO and this is now mentioned in the text. Of course water mass propagation might influence all areas, and this is mentioned now in the concluding remarks.

Secs. 3.2-3.4: If the authors are to extract decadal variability superimposed on the long-term trend (Sec. 3.1), it is better to examine the time series after subtracting the long-term trend.

Reviewer 3 proposed to go the opposite direction, remove first the PDO, NPGO and other climate trends before computing the long-term trend. The long-term trends might not be only related to ocean warming but also the PDO and other climate signals. Hence removing the long-term trend first might remove also the contribution by PDO and other signals, therefore we did not remove the long-term trend first and computed the PDO signal related to the observed oxygen and nutrient changes. For a time series of significant lengths, with several oscillations of the overlying signal this certainly would be the best approach, but since the data time series is short, any long term trend

certainly is influenced by the phase of the oscillation at the beginning and end of time series, thus making this approach less ideal.

Reply to reviewer 3

(our response **in bold font**)

We thank the reviewer for the helpful comments.

What is new in this manuscript (ms)? It is difficult to determine how much is original. The authors have completed an excellent synthesis of many data sources over many decades. This manuscript covers changes in four ocean properties in seven ocean areas and compares these changes to five climate indices and the global ocean surface temperature, providing more than one hundred possible relationships to be presented and evaluated.

I ask the authors to examine years with sparse data to determine how representative and accurate they might be. For example, if oxygen and nutrients vary in the opposite direction, does this relationship hold in years of sparse data? If changes in nutrients are in the same direction, then does this relationship hold in years of sparse data?

We are not sure if we understand the request of the reviewer here. Intra annual or short term variations in oxygen and nutrients can have a very different origin than long term variability, and they are not necessarily connected. Such an analysis, while interesting, would be possible for areas with sufficient data like CalCOFI, though we think the focus of the present manuscript should be on longer term changes. As the reviewer said, with already many options we decided to exclude the STCs to focus more on larger-scale correlations.

Why not plot the standard error of the mean values of oxygen and nutrients for each year? These standard errors might provide visual insight into the impact of years of sparse data on the trends and correlations.

Despite a simple task at glance, the data processing and in particular gathering was programmed in a way to bin data into annul data point early in the progress during data acquisition. To accommodate this desirable extension, we would have to change the computation of all areas used. Due to the often low amount of available data we combined all available data from one year into one profile which leads to a different amount of data points at different depth layers at different years and the error bars would not be comparable. A better option would be to no bin the data and work with the raw data, applying statistics that can handle highly heterogeneous data distributions, though this would make the data handling significant more complicated to follow, with no gain for the outcome and results. For more localized studies this would probably be justified, putting more emphasize on the study of regional variability.

Data deemed unacceptable by Schmidko et al. (2017) are included in this ms to avoid discarding already sparse data. The ms notes possible errors in density that might arise from including these data but does not give expected errors in oxygen or nutrients. Nor do they explain why errors in density are relevant to this ms.

We rewrote the text to describe in more detail why this was done and is justified from our point of view. The text now reads:

Quality control and handling is described in Schmidtko et al. (2017) for oxygen and used here similarly for nutrients. The only divergence to the described procedure was that bottle data with missing temperature and/or salinity were assigned the temporal and spatial interpolated temperature and salinity derived from MIMOC (Schmidtko et al., 2013). This was done to ensure all data were in µmol kg^{-1} and not requiring the discarding of already sparse data. In Schmidtko et al. (2017) this was not performed, since the error introduced near or in boundary currents and fronts can be significant. In contrast the areas here are chosen to represent homogeneous patches with significant amount of data in the open ocean, thus in the areas analyzed here, this may only lead to minor errors in density resulting in an error of less than 0.05%, therefore negligible small in µmol kg^{-1}, compared to the oxygen or nutrient data accuracy

In calculating correlations among time series, how are the number of degrees of freedom determined? Convince the readers that the number of degrees of freedom are determined appropriately.

As requested by reviewer 1 we modified the text explaining how the effective degrees of freedom were derived.

I prefer that the title state that the manuscript gives results for "... the depth range of 50 to 300 metres in selected areas of the North and equatorial Pacific". As for "influence of decadal oscillations on : : : trends", the trends over the full time series as shown in figures 3, 4, 5, and 7 do not take into account the impact of PDO and NPGO decadal signals on these trends from the 1950s to recent years. I believe the variability in the oxygen and nutrient time series related to PDO, NPGO and other climate decadal oscillations should be removed from the data before 50 to 70-year trend is determined. Such an adjustment would allow the manuscript to match its title.

Reviewer 2 proposed to go the opposite direction, remove first the long-term trend before computing the PDO and NPGO trends. The PDO and NPGO trends might contribute to the long-term trend. Hence removing the PDO and NPGO trends first might also remove the contribution to the long-term trend, therefore we did not remove the PDO and NPGO trends first and computed the different trends from the original data set. We changed the title to now state the depth interval from 50-300 metres.

Why are graphs for Area P, Peru and Aloha in the Supplement, whereas graphs for other areas are in the ms? Please put them all together in the ms.

The figures all look similar, hence showing all figures, including now an additional area proposed by reviewer 2, in the main text would be redundant as the main information is in Table 1. For those interested in details of all areas can reference the supplement.

The years of two maxima and two minima seem to be close for the 18-year oscillation and the NPI. How correlated are these two series? Can their impacts be separated?

Different to the earlier version, we now use the same time period of the oxygen data sets which led to different results. The maxima and minima are close and cannot

always be separated depending on data coverage. However, the correlation of the 18.6 year oscillation is much weaker than the NPI and we think it is an interesting result that these two oscillations lead to quite different correlations, reasons for this can bethe shorter-time fluctuations in the NPI or the sensitivity to phase shifts in the oscillation. This is now stated in the text.

The names of all agencies that provide data and time series of indices need to be given, rather than only their Internet sites.

'The names of the agencies/universities are included in the paragraph data availability with the web-pages'

The writing in many places is sloppy and sometimes wrong. Too much information is included that clutters an already complex ms. I have given a few examples of these features below, but all authors need to read all the ms carefully to deal with this issue.

Here are examples of sloppy and sometimes incorrect writing.

The manuscript states on page 2, last paragraph, that increases in ocean surface temperature influence oxygen concentration through changes in solubility of oxygen and changes in convection of oxygen to subsurface layers. This sounds reasonable to me. However, the sentence beginning on page 3, line 16, attributes oxygen changes to solubility changes only. This attribution is then contradicted in the following sentences.

As we mentioned convection on page 3, we thought we do not need to list all components again on page 3. Now we included on page 3: '…changes in convection and thermocline depth'. We also removed STC analysis from the manuscript to focus more on the indices with larger impacts.

On page 3 line 20, the ms notes that shoaling thermoclines during La Niña or cool (negative) PDO in the eastern Pacific enhance nutrient supply. Should this region be stated more accurately as eastern tropical Pacific? I expect there are regions of the eastern Pacific outside of the eastern tropical Pacific that behave otherwise during La Niña and negative PDO.

The eastern Pacific was mentioned at the beginning of the sentence, however to make it more clear that the related changes appear in the eastern Pacific we added ‘ in the eastern Pacific’ in the sentence mentioned as well as in the next sentence.

I was surprised by the definition of PDO as given on page 4 lines 21 to 23. It has been taken incorrectly from Dressler et al. (2010).

We assume Dressler et al. (2010) should be Deser et al. (2010). According to the definition of Deser et al. (2010) one word was missing, which is included in the revised version.

I believe the correct definition of El Nino and La Nina is “five consecutive 3-month periods ..” (page 6, line 3).

Various definitions of El Nino and La Nina do exist, the three months running mean was mentioned at the beginning of the sentence, however to make the definition more clear we modified the text as requested.

On page 11, line 14, the sentence reads “: : :the linear trend of the oxygen content of the layer 50 to 300 m decreases for the entire time period : : :” Actually, the linear trend is constant and negative. The trend would not be linear if it decreased.

Thanks for this information, ‘decreases’ is now replaced by ‘is negative’

I doubt that Station P was occupied continuously from 1943 and it was likely established as a weather observation site rather than an ocean measurement site. (page 7, line 13)

The description of Station P was taken from Wikipedia and is an example that in short summaries in Wikipedia wrong information might be included. Thanks for letting us know. Now the text reads:

Station P, located at 50°N, 145°W in the North Pacific, was established as a weather observation site with a weather ship in 1949 which was manned continuously until 1981, and routinely hydrographic measurements were started in the 1950's. After the termination of the weather ship program shipboard measurements were made on average 3 times a year since.

Solid lines in Figures 3, 5, etc, are described in the captions as representing positive PDO phase after 1977, despite the obvious negative phase from 1998 to 2012.

As the data base for nutrient measurements is small compared to oxygen and temperature measurements especially in regions with no continuous measurements, we think that another subdivision would stress the data set too much. As written in the text in the areas E and D the nutrient data base is so low, that we did not show the nutrient figures. For the area 2-5°S 84-87°W (Fig. 4) only two measurements are available for the period 1998 to 2013 and in the Peru region (now Suppl. Fig. S6) there is a data gap between 1985 and 2008. Hence we decided to define the entire period after 1977 as positive PDO in the text and the figure legends refer to the definition used for this manuscript.

Insert names of areas into the graphs of Figures 3 and 4. Give the units of ocean properties in Figures 4, 5, and 7, as well as the units of trends. Lines in gray on figures will be more visible if black is used.

The names Area E,D and G are now included in figures 3 and 4. Units for the parameters are given now in the figure legends of figures 4, 5, 7 as well as S3 to S6 as: (in µmol kg^{-1}, red crosses) while the units for the trends were already mentioned in the figure legends. Yes black lines for the PDO are more visible, but as the PDO curve is

just background information, we think that the PDO as black line dominates the figure too much (see figure below).

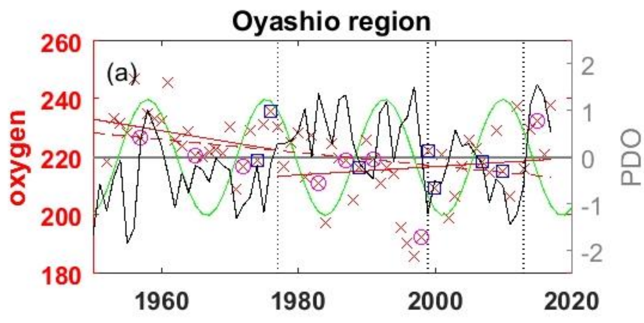

Examples of too much information:

I prefer that the Abstract begin with "Oxygen and nutrient time series since the 1950s were investigated at 50 to 300 metres depth in seven areas of the North and equatorial Pacific ..." The sentences preceding this one in the present Abstract are not necessary and divert the reader from the essential content of this manuscript.

According to the Geosciences guidelines for authors for the abstract: 'After a brief introduction to the topic, the summary recapitulates the key points of the article and mention possible directions for prospective research.' We prefer to start with an introduction instead of starting right away with the results.

The paragraph on page 11 from lines 11 to 18 notes the many areas in which the linear trend decreases for the entire time period. (I assume the trend is negative rather than decreasing). However, the final sentence notes that oxygen trends are not significant for the entire time period except in two areas. Why describe insignificant trends at all? There are sufficient significant trends to provide enough information to overwhelm most readers.

As requested by reviewer 1 significance should be avoided and the decision of good or bad should not be related to one fixed value. Hence we mention now only that areas are within or out of the 95% confidence interval.

The first 9 lines of page 12 describe numerical differences between this ms and previous studies. However, the depth ranges are different, and the years are different in the two studies. The information is not useful unless the differences are attributed to the depth range or years. This paragraph could be eliminated.
As earlier investigations in this region exist it seems reasonable to mention these results. Despite the different depth layers the comparison with earlier investigations indicates that changes are related to time periods analysed and not just a linear trend. This in now explained in more detail in the text. The bi-decadal trend is no longer mentioned in the respective paragraph as this is the subject of the later paragraph.

Regarding the subtropical convergence cell (STC), on page 16, lines 10-13, the authors note that, “Due to the long duration of the STC phases and the sparse data set, it is not possible to perform a meaningful correlation analysis to investigate STC influence on the oxygen and nutrient variations.” In addition, the authors note on page 20, line 20, that the STC showed no clear signal in the equatorial Pacific. Given this lack of impact, why devote any text to the STC at all, except to say it does not have significant correlation with oxygen and nutrient time series, despite an expectation that it might?
The reviewer is correct; we now exclude the analysis of STCs in the manuscript to focus more on the indices with large-scale impact. This made the manuscript more focused and the reader is hopefully less distracted by indices that we do not find to correlate significantly.

List of relevant changes made in the manuscript:

The title of the manuscript was changed (see below) according to a comment by reviewer 3 and the new title fits the derived results much better.

The changes made according to the reviewers comments are visible in the following marked manuscript and the marked supplement.

~~The influence of decadal oscillations on the oxygen and nutrient trends in the Pacific Ocean~~

Trends and decadal oscillations of oxygen and nutrients at 50 to 300 m depth in the North and Equatorial Pacific

Lothar Stramma[1], Sunke Schmidtko[1], Steven J. Bograd[2], Tsuneo Ono[3], Tetjana Ross[4], Daisuke Sasano[5], and Frank A. Whitney[4]

[1]GEOMAR Helmholtz Centre for Ocean Research Kiel, Düsternbrooker Weg 20, 24105 Kiel, Germany

[2]Environmental Research Division, Southwest Fisheries Science Center, NOAA, Monterey, California, USA

[3]National Research Institute for Far Sea Fisheries, Fisheries Research and Education Agency, 2-12-4 Fukuura, Kanazawa-Ku, Yokohama 236-8648, Japan

[4]Institute of Ocean Sciences, Fisheries and Oceans Canada, PO Box 6000, Sidney BC V8L 4B2, Canada

[5]Global Environment and Marine Department, Japan Meteorological Agency, Tokyo, Japan

Correspondence to: Lothar Stramma (lstramma@geomar.de)

Abstract. A strong oxygen deficient layer is located in the upper layers of the tropical Pacific Ocean and ~~at~~ deeper ~~depths~~ in the North Pacific. Processes related to climate change (upper ocean warming, reduced ventilation) are expected to change ocean oxygen and nutrient inventories. In most ocean basins, a decrease in oxygen ('deoxygenation') and an increase of nutrients has been observed in subsurface layers. Deoxygenation trends are not linear and there could be ~~other~~ multiple influences on oxygen and nutrient trends and variability. Here oxygen and nutrient time series since 1950 in the Pacific Ocean were investigated at 50 to 300 m depth, as this layer provides critical pelagic habitat for biological communities. In addition to trends related to ocean warming the oxygen and nutrient trends show a strong influence of the Pacific Decadal Oscillation (PDO) in the tropical and the eastern Pacific, and the North Pacific Gyre Oscillation (NPGO) especially in the North Pacific. In the Oyashio Region the PDO, the NPGO, the North Pacific Index (NPI) and a 18.6 year nodal tidal cycle overlay the long-term trend. In most eastern Pacific regions oxygen increases and nutrients decrease in the 50 to 300 m layer during the negative PDO phase, with opposite trends during the positive PDO phase. The PDO index encapsulates the major mode of surface temperature variability in the Pacific and oxygen and nutrients trends throughout the basin can be described in the context of the PDO phases. ~~An influence of the subtropical-tropical cell in the tropical Pacific cannot be proven with the available data.~~ El Niño and La Niña years often influence the oxygen and nutrient distribution during the event in the eastern tropical Pacific, but do not have a multi-year influence on the trends.

1 Introduction

Oxygen and nutrient distribution are key parameters controlling marine ecosystems. How oxygen and nutrient concentrations vary and co-vary ultimately controls biogeochemical cycles. Globally, oxygen has been estimated to have decreased in the ocean by 2% during the past five decades, likely caused by climate change related temperature increases, with the largest oxygen decrease in the North and equatorial Pacific (Schmidtko et al., 2017). Increasing sea surface temperatures reduce~~s~~ the solubility of oxygen in sea water and increase~~s~~ stratification which leads to less convection of oxygen rich water to subsurface layers. The global mean surface temperature (GISTemp) anomaly (e.g. Hansen et al., 2010) shows an increase of about 0.3°C from early 1900 to 1950, stagnant values between 1950 to 1976 and an increase of about 0.8°C from 1976 to 2015 (Fig. 1). Results from the UVic ECSM (University of Victoria Earth System Climate Model) model indicate that ocean oxygenation varies inversely with low-latitude surface wind stress (Ridder and England 2014).

In the tropical eastern Pacific, two subsurface low-oxygen zones exist north and south of the equator, with a pronounced minimum in oxygen at ~100 to 500 m depth, and are referred to as oxygen minimum zones (OMZ's) or oxygen deficient zone (ODZ's). These OMZ's are suboxic (oxygen concentrations below ~4.5-10.0 µmol kg^{-1}; e.g. Karstensen et al., 2008; Stramma et al., 2008). In suboxic regions, nitrate and nitrite become involved in respiration processes such as denitrification or anammox (e.g. Kalvelage et al., 2013). Decreasing and, in few areas of the Pacific, increasing oxygen content in the OMZ layer over the last 50 years has been described (e.g. Stramma et al., 2010). In the subarctic North Pacific surface nutrient concentration decreased during 1975 to 2005, and is strongly correlated with a multidecadal increasing trend of sea surface temperature (SST) (Ono et al., 2008). Below the surface, however, oxygen decreased and nutrients increased in the subarctic Pacific pycnocline from the mid-1980s to around 2010 (Whitney et al., 2013). Nutrients would be expected to vary inversely with oxygen, if the dominant process was the remineralization of marine detritus (Whitney et al., 2013).

Climate modes influence oxygen and nutrient distributions. Because of the influence of SST on the solubility of oxygen, changes in convection and thermocline depth the most prominent control on oxygen changes in the Pacific might be exerted by the Pacific Decadal Oscillation (PDO). A shoaling thermocline, such as occurs in the eastern Pacific during La Niña or cool (negative) PDO state, enhances nutrient supply and organic matter export in the eastern Pacific while simultaneously increasing the fraction of that organic matter that is respired in the low-oxygen water of the uplifted thermocline. The opposite occurs during El Niño or a warm (positive) PDO state; a deeper thermocline reduces both export and respiration in low-oxygen water in the eastern Pacific, allowing the hypoxic water volume to shrink (Deutsch et al., 2011; Fig. S7). Previous syntheses of tropical and North Pacific physical, biological and chemical conditions during warm and cold PDO regimes have shown the far-reaching influence of the PDO on the Pacific Ocean, for example in controlling the out-of-phase relationship between sardine and anchovy populations in the eastern Pacific (Chavez et al., 2003). In a pattern similar to the PDO SST during the warm regime, lower nutrients are shown for the eastern equatorial and near-coastal tropical Pacific and higher nutrients in the northern Pacific, and vice-versa for the cold regime (Chavez et al., 2003; their Fig. 3). A similar relationship to the PDO was also observed for surface (5-10 m) nutrient concentrations in the North Pacific (north of 10°N, Yasunaka et al. 2016). Model simulations for the eastern Pacific Ocean for typical PDO positive conditions show a volume expansion of the suboxic regions by 7% in 50 years due to a slow-down of the large scale circulation related to the decrease of the intensity of the trade winds (Duteil et al., 2018). Other climate modes that could influence the oxygen and nutrient trends are the North Pacific Gyre Oscillation (NPGO; Di Lorenzo et al., 2008),~~ the Pacific subtropical-tropical cell (STC; e.g. Duteil et al., 2014)~~, the North Pacific Index (NPI) and El Niño-Southern Oscillation (ENSO) events.

Here we use publicly available oxygen and nutrient data augmented with recent ship data to investigate the influence of decadal climate oscillations on the oxygen and nutrient variability in the tropical, eastern and northern Pacific Ocean where long time series are available. For the negative PDO phase we use data between 1950 and 1976. As there are large data gaps in the 1990s and early 2000s we use data since 1977 for the warm PDO despite the variable PDO conditions after 1998. In addition, a possible influence of the NPGO, of the NPI,~~the STC,~~ of ENSO and of a 18.6 year oscillation (Royer 1993) in the North Pacific ~~is~~ are investigated.

2 Climate signals and data sets

2.1 Climate signals

Several climate signals are investigated here with regard to a possible influence on the oxygen and nutrient distribution and some basic details are listed here.

The PDO is the leading empirical orthogonal function (EOF) of monthly SST anomalies over the North Pacific between 20°N and 70°N, after removing the global mean SST anomaly and its associated principal component (PC) time series (Mantua et al., 1997; Deser et al., 2010; Newman et al., 2016). The temperature pattern and the PDO time series (Supplement Fig. S1) show that the PDO was negative during 1944 to 1976 with a stagnant temperature period, and warming temperatures since 1977 with PDO positive during 1977 to 1998 and PDO variable after 1998. At the time of transition from negative to positive PDO a climate shift in the eastern and central North Pacific Ocean occurred in 1976-77, which was caused by unique atmospheric anomalies acting over several months before the 1976-77 winter (Miller et al., 1994). Despite a positive PDO index from 2002 to 2006 (Fig. 1), the period 1998 to 2013 is dominated by negative seasonal mean PDO indices and is typically considered as a cool (negative PDO) phase (Trenberth 2015).

The North Pacific Gyre Oscillation (NPGO) index tracks the changes in strength of the central and eastern branches of the North Pacific gyres and of the Kuroshio-Oyashio Extension. Like the PDO, it is a mode of decadal climate variability and it is defined as the second dominant mode of variability in sea surface height anomaly in the northeast Pacific over the region 180-110°W, 25-62°N (Di Lorenzo et al., 2008). Subsurface nutrient variability in the Gulf of Alaska, Line P in the eastern North Pacific at about 50°N and the California Current System have been shown to be correlated with the NPGO (Di Lorenzo et al., 2009).

~~A decadal decline of the Pacific subtropical cells (STC) from the 1950s into the 1990s was computed between 9°N and 9°S with a decreased equatorward convergence of 12 Sv (McPhaden and Zhang 2002). This was followed by an increase of STC convergence from the mid 1990s to about 2000 (McPhaden and Zhang 2004). The transport changes observed in the Pacific STC (e.g. Schott et al., 2008), with a decrease of 30% from the 1960s to the 1990s, resulted in reduced transports of oxygen~~

~~and phosphate to the tropics in model simulations (Duteil et al., 2014). In model computations the decadal variability of STC in the Northern Hemisphere was found to be strongly associated with the PDO while in the south the STC only passively responds to the PDO (Hong et al., 2014).~~

In the North Pacific, the NPI (North Pacific Index; anomaly of the sea surface level pressure in the wintertime of the North Pacific (160°E-140°W, 30°N-65°N; Minobe, 2000) was introduced. In observations in the Northwest Pacific a bi-decadal oscillation related to minima in 1962 and 1983 and maxima in 1971 and 1991 (Watanabe et al., 2003, their Fig. 2) has been described.

The ENSO cycle of alternating warm El Niño and cold La Niña events is the climate system's dominant year-to year signal. ENSO originates in the tropical Pacific through interaction between the ocean and the atmosphere, but its environmental and socioeconomic impacts are felt worldwide (McPhaden et al., 2006). Three month running mean sea surface temperature anomalies (ERSST.v5 SST anomalies) in the Niño 3.4 region (equatorial Pacific: 5°N to 5°S, 120°W to 170°W) of at least +0.5°C and lasting for at least 5 consecutive three months periods are defined as El Niño events and 5 consecutive three months periods of at least -0.5°C are defined as La Niña events (http://origin.cpc.ncep.noaa.gov/products/analysis_monitoring/ensostuff/ONI_v5.php). In the eastern Pacific, ENSO variability is most pronounced along the Equator and coastal Ecuador, Peru and Baja California (Wang and Fiedler, 2006). Coastal warming during El Niño is caused by downwelling Kelvin waves generated by mid-Pacific westerly wind anomalies that deepen the eastern thermocline, nutricline and oxycline and allow warming to occur (Kessler, 2006). Consequently, during El Niño events the upwelled water off the coast is warmer, more oxygen replete and less nutrient-rich while during La Niña events the water is colder, oxygen poor and nutrient-rich (e.g., Graco et al., 2017).

2.2 Data Sources by Regions

The main hydrographic dataset is similar to the one used and described in Schmidtko et al. (2017), relying on Hydrobase and World Ocean Database bottle data for nutrient data. Quality control and handling is described in Schmidtko et al. (2017) for oxygen and used here similarly for nutrients. The only divergence to the described procedure was that bottle data with missing temperature and/or salinity were assigned the temporal and spatial interpolated temperature and salinity derived from MIMOC

(Schmidtko et al., 2013). This was done to ensure all data were in µmol kg^{-1} and not requiring the discarding of already sparse data. In Schmidtko et al. (2017) this was not performed, since the error introduced near or in boundary currents and fronts can be significant. In contrast the areas here we~~a~~re chosen to represent homogeneous patches with significant amounts of data in the open ocean, thus in the areas analyzed here,~~: bottle data with missing temperature and/or salinity were assigned the temporal and spatial interpolated temperature and salinity derived from MIMOC (Schmidtko et al., 2013).~~ t~~T~~his may only lead to minor errors in density ~~on the order of ~0.5 kg m^{-3}, thus~~resulting in an error of ~~about~~ less than 0.05%, therefore negligible small in µmol kg^{-1}~~.~~, compared to the oxygen or nutrient data accuracy. Similarly, a nutrient file was compiled (status 25 February 2019). This compilation of hydrographic, oxygen and nutrient data are referred to in the following as ‘hydrodata’. The final hydrodata set was used to extract data for our regions of interest.

As nutrient data are sparse in many regions of the Pacific, areas were selected due to their better temporal data coverage (most regular sampling over the longest time period). Three regions in the equatorial Pacific were selected which can be compared with earlier observations. In the equatorial region mainly hydrodata were used. The region at 5°N-5°S, 165°-175°W (area E in Stramma et al., 2008; shown in Fig. 2a) which had hydrodata until 2009, was supplemented with data from a *R/V Investigator* cruise at 170°W from June 2016. The region 5°N-5°S, 105°-115°W (area D in Stramma et al. 2008; shown in Fig. 2a), which had hydrodata until 2008, was supplemented with data from a RV *Ron Brown* cruise at 110°W in December 2016. The area 2°S-5°S, 84°-87°W (near the Galapagos Islands, marked in Fig. 2a as area G) had been used by Czeschel et al. (2015) to investigate nutrient trends and is supplemented here with recent cruises until 2017.

Off California, intense repeated measurements have been made since 1949 within the California Cooperative Oceanic Fisheries Investigations (CalCOFI) project and data from the bottle data set (downloaded from http://www.calcofi.org/ccdata.html, status 13 August 2018; data period March 1949 to November 2017, however with sparse nutrient data prior to 1984) were used to investigate the oxygen and nutrient changes within the California Current. We use the CalCOFI 1x1° data subset at 34-35°N, 121-122°W without additional hydrodata and no additional historic nutrient data. This region is located near the center of the CalCOFI station grid and we referred to it as CalCOFIc (shown in Fig. 2a).

Station P, located at 50°N, 145°W in the North Pacific, ~~is an ocean measurement site~~ was established as a weather observation site with a weather ship in 1949~~3~~ which was manned continuously until 1981, and routinely hydrographic measurements were started in the 1950's. After the termination of the weather ship program shipboard measurements were made ~~and then~~ on average 3 times a year since. The data set from the Institute of Ocean Sciences, Sidney BC, Canada covers (status September 2018) the time period May 1956 to August 2017 with data collected on research cruises. The Station P data were supplemented here by hydrodata in the surrounding region 48°-52°N, 143°-147°W, which we refer to as area P (shown in Fig. 2a) in the following.

The Hawaii Ocean Time-series for the region north of Hawaii was taken from hydrodata in the region 22-25°N, 156-159°W and downloaded bottle data for the Aloha station at 22°45'N, 158°W (http://hahana.soest.hawaii.edu/hot/hot-dogs/bextraction.html status 15 January 2019, time period covered October 1988 to December 2017). This data set is called Aloha region (shown in Fig. 2a) in the following. Different to the other regions this station is located in the subtropics with high oxygen content and low nutrient concentrations in the subsurface layer (Fig. 2). As there were continuous measurements since the 1980s we included this region in our investigation.

The measurements in the Oyashio region east of Japan (39°-42°N, 144°-149°E; shown in Fig. 2a)) are from hydrodata, augmented with updated data collections used in Whitney et al. (2013). Hydrographic and biogeochemical measurements have typically been made in this region in every season since 1954 (used in Sasano et al., 2018) and were included here up to 2017.

For fifty years a repeat section was covered in the western Pacific along 137°E (Oka et al., 2018). The section was measured biannually in winter and summer. To cover the western tropical Pacific an area 20°-26°N, 134°-140°E was selected from the hydrodata and added with nutrient data for the period 2008 to 2018 from the 137°E section as the hydrodata does not cover the period after 2008.

In the eastern tropical Pacific (2°S-5°S, 84°-87°W; area G) and off Peru (7-12°S, 78-83°W; called Peru region in the following) the hydrodata could be extended with some RV *Meteor* cruises carried out across the equator and near the Peruvian coast, with two cruise legs from December 2008 to February 2009 (M77/3 and M77/4; Czeschel et al., 2011), in November 2012 (M90; Stramma et al., 2013) at 85°50'W and in June 2017 (M138). Sections across the Peruvian shelf between 9°S and 16°S were made during RV *Meteor* cruise M91 in December 2012 (Czeschel et al., 2015) and M135 in March 2017. In October 2015 an RV *Sonne* cruise from Guayaquil, Ecuador to Antofagasta, Chile, was carried out with sections at the equator and off the shelf of Peru (Stramma et al., 2016). Although these measurements were made during one of the strongest El Niño events since the 1950s, the October 2015 measurements are used for the trend computations to estimate the influence of the El Niño event. In the figures the El Niño events of 1982/83, 1997/98 and 2015/16 are defined as very strong El Niño events and the strong El Niño events (1957/58, 1965/66, 1972/73, 1987/88 and 1991/92) are marked by circles and the strong La Niña events (1973/74, 1975/76, 1988/89, 1998/99, 1999/2000, 2007/08 and 2010/11) are marked by squares in these years.

2.3 Data Processing

On ~~the~~ recent cruises the CTD oxygen sensors were calibrated with oxygen measurements obtained from discrete samples from the rosette applying the classical Winkler titration method, using a non-electronic titration stand (Winkler, 1888; Hansen, 1999). The root mean square uncertainty of the CTD oxygen sensor calibration was on the order of ±1.0 μmol kg^{-1}.

Nutrients nitrite (NO_2^-), nitrate (NO_3^-), phosphate (PO_4^{3-}) and silicic acid ($(Si(OH))_4$ referred to as silicate hereafter) on the recent cruises were measured on-board with a QuAAtro auto-analyzer (Seal Analytical). For recent autoanalyzer measurements precisions are 0.01 μmol kg^{-1} for phosphate, 0.1 μmol kg^{-1} for nitrate, and 0.5 μmol kg^{-1} for silicate and 0.02 mL L^{-1} (~ 0.9 μmol kg^{-1}) for oxygen from Winkler titration (Bograd et al., 2015). For older uncorrected nutrient data, offsets are estimated to be 3.5% for nitrate, 6.2% for silicate and 5.1% for phosphate (Tanhua et al., 2010).

To investigate oxygen and nutrient trends we use the hydrodata set and recent ship sections to construct time series of annual mean oxygen and nutrient profiles. Oxygen and nutrient data are presented in μmol kg^{-1}, with data obtained in different units converted to μmol kg^{-1}. Linear trends and their ~~95%~~

~~confidence interval~~statistical significance were computed using binned annual ~~averages~~ data ~~(all measurements from one year were attributed to that year, as in earlier investigations; e.g. Czeschel et al., 2015)~~ of the ~~profiles~~ linearly standard depth interpolated profiles ~~to standard vertical depth levels~~ (all measurements from one year were attributed to that year, as in earlier investigations; e.g. Czeschel et al., 2015). This wa~~i~~s done since intra-annual variability is small compared to the inter-annual variability and the modes analysed are of greater time spans, the reduction of data clusters greatly reduces the possible systematic bias in the trends. We do not address the errors in the vertical interpolation on standard depths, because the layer analysed is thin and characterized in general by a linear decrease/increase in observed values. Due to heterogeneous vertical sampling the error is assumed to be small compared to the observed inter-annual variability. For the trend computation, ~~S~~successive years of the time series are not necessarily statistically independent of each other. Therefore we determined ~~a computation routine was used which used~~the effective number of degrees of freedom for the computation of the confidence interval. For each time series the lag dependent temporal half folding range of the autocorrelation function was used to compute the degrees of freedom. The length of the time series was divided by the length of the time derived from the autocorrelation function, giving a statistical measure of the degrees of freedom for each analysed time series independently.

As historical measurements are focussed on the upper ocean and as oxygen and nutrient changes will have the largest impact on the biology in the upper ocean, the trends have been computed for the subsurface layer 50 to 300 m as presented in Czeschel et al. (2015). The upper boundary at 50 m was selected to avoid influence from atmosphere-ocean interaction in the mixed layer. In the North Pacific seasonal variability will reach below 50 m depth. The two areas we consider in the North Pacific contain a lot of data and a test omitting the winter months measurements (January to March: Supplementary Table S1) shows similar trends as for the entire year (Table 1), hence the seasonal cycle did not have a larger impact on the results. The oxygen and nutrient distribution at 50 to 300 m depth (Fig. 2) shows the large variation of the parameters across the Pacific. The subtropical gyres are clearly visible by enhanced oxygen and low nutrient content. Higher nutrients are seen in the equatorial and eastern Pacific in the areas of equatorial and coastal upwelling, respectively. As gradients are low in regions of low nutrient content and nutrient data are often sparse, it makes sense to investigate changes in regions with enhanced nutrient content and a sufficiently long time series.

The data used for the oxygen and nutrient time series were interpolated with an objective mapping scheme (Bretherton et al. 1976) with Gaussian weighting using a temporal half folding range of 0.5 years and a vertical~~spatial~~ one of 50 m, a maximum temporal range of 1 year and spatial range of 100 m. The covariance matrix was computed from nearest 100 local data points and 50 randomly distributed data points within the maximum range, for the diagonal of the covariance matrix a signal to noise ratio of 0.7 was set (see Schmidtko et al. 2013, for details). Due to the random data points the computed trends and confidence intervals vary slightly in each computation run of the interpolation, however the variation is very small compared to the confidence interval.

The correlation coefficient and significance between the oxygen time series and the PDO or NPGO were computed for all~~the~~ years available~~fter 1976~~,~~ using the MatLab routine corrcoef~~ using a chi-squared test with the degrees of freedom as computed above. Often~~and~~ the correlation was considered as significant for 95% confidence interval different from null~~for a P-value ~<0.05~~, however recently it is stated that it seldom makes sense to calibrate evidence as a function of p-values (McShane et al., 2019) and it was suggested to retire the term statistical significance and only state direct p-values (Amrhein et al., 2019). In the following we list the p-value of the null hypotheses in parentheses. For some regions with a longer time series the correlation was also computed for temperature or nitrate. In the North Pacific the correlation of oxygen with a 18.6 year oscillating signal were computed for the entire period with existing oxygen data~~ after removing the derived long-term trends~~. To investigate the lag the measurement years were shifted from -15 to +15 by 1-year steps. Since the PDO or NPGO time series are continuous, data point reduction due to lag shift are small and only occurring for individual data collected in the last 15 years. The impact is assumed to be smaller than the here given uncertainties.

3 Trends and influence of climate signals

3.1 Long-term trends

In the global ocean the long-term surface temperature trend 1901-2012 was positive everywhere except for a region in the North Atlantic (IPCC 2013, Fig. 2.21). However, for 1951 to 1980 decreasing surface temperatures were reported across the North Pacific Ocean (IPCC 2013, Fig. 2.22). For 1981 to 2012, while the western Pacific showed a warming trend, a large region with decreasing surface temperatures was seen in the eastern Pacific Ocean. However, a different pattern emerges when the analysis is applied to the subsurface layer (50 to 300 m). Subsurface temperature trends computed for all data since 1950 in each of the regions discussed in section 2, showed weak~~ and not significant~~ temperature increases. Exceptions are 1) the area P with a~~ significant~~ temperature increase in the 95% confidence interval of 0.0083 ± 0.0073°C yr^{-1} for the period 1954 to 2017, with the highest temperatures in the positive PDO periods 1977 to 1999 and since 2013, and 2) the Oyashio region, where a strong~~ and significant~~ temperature decrease in the 95% confidence interval of -0.0273 ± 0.0188°C yr^{-1} was derived for the period 1952 to 2017 with the lowest temperatures in the period 1977 to 2010 (Suppl. Fig. S2). This agrees with the surface layer (0 to 50 m), where all areas showed increasing temperature for the entire measurement period, except for the Oyashio region where temperature decreased (Suppl. Fig. S2). The very strong temperature increase at area P after 2013 was impacted by the strong surface temperature anomaly in the Northeast Pacific Ocean during 2013 to 2015 marine heatwave nicknamed The Blob (Bond et al., 2015: Di Lorenzo and Mantua, 2016). For the subsurface layer discussed here, however, it appears that the marine heatwave peaked in 2016-2017 (Jackson et al., 2018). Except for the Aloha and the CALCOFIc regions all 0 to 50 m trends were not within the 95% confidence interval~~significant~~, probably due to interdecadal, seasonal and regional variations in the temperature measurements. The temperature trends are in agreement with the sea surface temperature expression of the PDO (Suppl. Fig. S1), which is positive in the area P region and strongly negative in the Oyashio region.

In the open ocean a decline in mean oxygen solubility of ~5 µM associated with a hypothetical warming of 1°C throughout the upper ocean would expand the reach of hypoxic conditions by 10% while suboxic zones would nearly triple in volume (Deutsch et al., 2011). However the sensitivity of hypoxic zones to variations in the depth of the thermocline introduces a mechanism for counteracting this expansion (Deutsch et al., 2011). In the areas of the equatorial Pacific (Fig. 3 and 4), the CalCOFIc region off California (Fig. 5), the area P in the North Pacific (Suppl. Fig. S3), the Aloha region north of Hawaii (Suppl. Fig. S4), the Oyashio region in the western North Pacific (Fig. 7) and a region off Peru (Suppl. Fig. S6~~5~~), the linear trend of the oxygen content of the layer 50 to 300 m is negative~~decreases~~ for the entire time period of available data since 1950, except for the 137°E data between 134° and 140°E in the western Pacific (Suppl. Fig. S5) and the eastern equatorial region 2° to 5°S, 84° to 87°W (just northwest of the Peru region) which has a positive trend caused by low and variable oxygen content in the 1955 to 1965 period. However, except for the western equatorial areas and area P, the oxygen trends are not within the 95% confidence interval~~significant~~ with regard to the entire time series (Table 1).

The long-term trends of the western equatorial regions between 5°N and 5°S at 165°-175°W and 105°-115°W show a continuous oxygen decrease since 1950 for the 50 to 300 m layer of -0.36 ± 0.22 µmol kg^{-1} yr^{-1} and -0.65 ± 0.37 µmol kg^{-1} yr^{-1} (Fig. 3; Table 1). These trends are larger than the trends for the same regions since 1960 for the 300 to 700 m layer of -0.19 ± 0.20 µmol kg^{-1} yr^{-1} and -0.13 ± 0.32 µmol kg^{-1} yr^{-1} (Stramma et al., 2008), as the deeper layer is located at the low oxygen core of the OMZ where no large changes are possible.

For the period 1956 to 2006 at area P in the depth range 100 to 400 m an ocean warming of 0.005-0.012°C yr^{-1} has been described (Whitney et al. 2007). Our longer temperature time series 1954 to 2017 at 50 to 300 m of 0.0083°C yr^{-1} confirms this trend (Suppl. Fig. S2). The oxygen trend of -0.24 ± 0.23 µmol kg^{-1} yr^{-1} in area P (48°-52°N, 143°-147°W) for the 50 to 300 m layer for 1954 to 2017 is smaller than that previously reported for area P at different depth layers between 100 and 400 m for the shorter time period 1956 to 2006 (0.39-0.70 µmol kg^{-1} yr^{-1}; Whitney et al., 2007). For yet another time period (1987 to 2011) and the layer 100-500 m in area P, trends have been reported (Whitney et al., 2013): -0.9 µmol l^{-1} yr^{-1} for oxygen (= density*µmol kg^{-1} yr^{-1}; ~0.88 µmol kg^{-1} yr^{-1}), 0.085 µmol l^{-1} yr^{-1} for nitrate, 0.30 µmol l^{-1} yr^{-1} for silicate and 0.0033 µmol l^{-1} yr^{-1} for phosphate). Our trends for 50 to 300 m for the longer time period 1977 to 2017 (Table 1) are much smaller for oxygen (-0.18 µmol kg^{-1} yr^{-1}) and slightly smaller for the nitrate (0.093 µmol kg^{-1} yr^{-1}), silicate (0.193 µmol kg^{-1} yr^{-1}) and phosphate (0.001 µmol kg^{-1} yr^{-1}).

The Aloha region is located in the southern part of the North Pacific subtropical gyre where oxygen is high and the nutrient inventory low. The oxygen trend since 1951 is negative although not in the 95% confidence interval~~significant~~. Nitrate and silicate trends (available since 1984/1985) are positive, while phosphate decreases. However, only the trends in silicate (including one measurement in 1970) and phosphate are within the 95% confidence interval~~significant~~ (Table 1).

For a region similar to our Oyashio region an oxygen decrease of 0.73 µmol kg^{-1} yr^{-1} between 1968 to 1998 has been reported for the density layer 26.8-27.4 kg m^{-3} (~260-1030 m)~~, superimposed with a bi-decadal trend of about 18 years~~ (Watanabe et al., 2003). Our oxygen trend for the layer 50 to 300 m is slightly positive (+0.15 µmol kg^{-1} yr^{-1}) for the period 1977-2017 and negative (-0.23 µmol kg^{-1} yr^{-1}) for the longer time period of 1952 to 2017. The phosphate increase in the deep layer 26.8-27.4 kg m^{-3} was reported as 0.004 µmol kg^{-1} yr^{-1} in Watanabe et al. (2003) while in our 50 to 300 m layer the phosphate trends for the positive and negative PDO periods and the entire period are larger, up to 0.010 µmol kg^{-1} yr^{-1} (Table 1). We observe a large silicate increase in the Oyashio region, +0.667 µmol kg^{-1} yr^{-1} since 1981 (Table 1). This exceptional silicate enrichment in the Oyashio region was noticed before and it was speculated that warming and a reduction of dense water formation causes this enrichment, because less silicate is transported into deep (>300 m) waters (Whitney et al., 2013). Despite the different depth layers the comparison with earlier investigations indicate that changes are related to time periods and not just a linear trend.

In the western Pacific at 137°E (20°-26°N) an opposite long-term trend compared to the Oyashio region was observed (Table 1). In the 50-300 m layer oxygen increased while nitrate, silicate and phosphate decreased (Suppl. Fig. S5). According to a map of oxygen changes in the upper 1200 m since 1960 (Oschlies et al., 2018; Fig 3a) this is a region with oxygen trends in the range -5 to +5 µmol kg^{-1} decade^{-1} hence the weak positive oxygen trend is possible in this region. Also the weak positive temperature trend (not shown) at 137°E is opposite to the negative temperature trend in the Oyashio region.

In the Peru region the oxygen, silicate and phosphate in the 50 to 300 m layer decrease while nitrate increases (Suppl. Fig. S6~~5~~). However, these long-term trends are not within the 95% confidence interval~~significant~~ (Table 1), possibly due to the paucity of data and the reversal of trends related to the PDO phases as described below.

The oxygen time series from most~~the different~~ Pacific regions~~ generally~~ show decreasing oxygen, although with varying magnitudes. These variations could be related to different climate signals as investigated below. The nutrient time series often show an increase over time: as expected, this is the opposite trend to oxygen.

3.2 The influence of the Pacific Decadal Oscillation (PDO)

An influence of the PDO has been seen in oxygen measurements (e.g. Czeschel et al., 2012) and modelling studies (e.g. Frölicher et al., 2009). According to the description of the PDO influence on the thermocline depth (e.g. Deutsch et al., 2011; Chavez et al., 2003) it is expected that during cold PDO phases the oxygen will decrease and the nutrients increase in the eastern equatorial and tropical Pacific, while during warm PDO periods the oxygen should increase and the nutrients decrease. However, visual inspection of the oxygen time series in the equatorial Pacific (areas E and D; see Fig. 2 in Stramma et al., 2008) indicates stagnant oxygen concentrations before 1976 during the cold PDO and enhanced oxygen depletion since the 1980's in the OMZ in the subsurface layer. The annual mean oxygen concentration for the layer 50 to 300 m for 5°S-5°N, 165-175°W (area E) and 5°S-5°N, 105-115°W (area D) show a strong oxygen decrease after 1976 (Fig. 3a and Fig. 3b). As nutrient data in the open Pacific are sparse, no reliable nutrient trends could be derived for areas E and D. The correlation of the PDO with the 50 to 300 m oxygen is high with p-values of ~ 0.001~~and significant~~ for all areas along the equator with the highest correlation coefficient of +0.83~~2~~ at 2~~5~~°S~~N~~ to 5°S, 84~~165~~°W to 87~~175~~°W (area G~~E~~) and slightly decreasing towards the we~~a~~st (Table 2).

Czeschel et al. (2015) showed decreasing oxygen and increasing nutrients in the 50 to 300 m layer of the area 2-5°S, 84-87°W (area G) since 1976. If PDO influence acts as expected, an even stronger gradient should exist prior to 1976. For the layer 50 to 300 m between 2°S and 5°S, 84°W and 87°W, for the post-1976 positive PDO period, the computed trend is slightly modified compared to the time period investigated in Czeschel et al. (2015). Here we see decreasing oxygen concentrations but increasing nitrate and phosphate and decreasing silicate concentrations since 1977 (Fig. 4). The main differences between these time series are improvements to the objective analysis, less smoothing being applied, and two more cruises added for 2015 and 2017. The resulting trends since 1977 for oxygen and nitrate are smaller, for phosphate larger~~ (though not significant)~~ and for silicate reversed compared to Czeschel et al. (2015). Oxygen for the negative PDO phase (1955 to 1976) showed a strong~~significant~~ positive trend of 1.63 ± 1.18 µmol kg^{-1} yr^{-1} for the 50 to 300 m depth layer in the area G which led to a small positive oxygen trend for the entire time period since 1955.

Near California the CalCOFIc bottle data in the region 34-35°N, 121-122°W (Fig. 5, Table 1) show similar trends as for the equatorial area (2-5°S, 84-87°W; area G) for the period since 1977, with decreasing oxygen and increasing nitrate, phosphate and silicate. The long-term trend over all measurements since 1950 show increasing nitrate and phosphate and decreasing oxygen and silicate for the CalCOFIc region similar to the long-term trends for the equatorial region. The correlation between the 50-300 m annual means and the PDO annual mean is 0.42~~4~~ (p=0.002) for oxygen (Fig. 6a; Table 2) and -0.3~~4~~7 (p=0.019) for nitrate (Table 2) for the period after 1976 with the PDO leading~~agging~~ by eleven~~one~~ years for oxygen.

For the area P (48°-52°N, 143°-147°W) the correlation with PDO is~~(~~ 0.30~~3~~ (p=0.019)~~;~~ (Table 2)~~ is not significant~~ for oxygen, and~~while~~ the correlation coefficients are~~of~~ -0.27~~38~~ (p = 0.109) for nitrate and~~ of~~ +0.46~~38~~ (p <0.001) for temperature (with the PDO lagging by 10~~2~~ years for oxygen)~~ are significant~~. It is~~Also~~ remarkable~~ is~~ that the trends in oxygen are unchanged, whether fitting to the entire record or to the positive and negative PDO time periods separately. Hence in this northern Pacific region the PDO has a weak influence on the 50 to 300 m biogeochemistry, probably caused by water masses propagating by 5 to 15 years from the Oyashio region into this part of the North Pacific (Ueno and Yasuda, 2003) while the correlation of the PDO and oxygen is larger in the other regions of the North Pacific.

The Aloha region is located at the transition of the warm and cold area of the PDO, thus one might expect the influence of the PDO to be weak in this region. However, the oxygen was observed to increase during cold PDO and the trend was close to zero in the warm PDO phase (Suppl. Fig. S4). During the PDO warm phase nitrate and silicate increased while phosphate decreased. There are too few nutrient data in the period of the PDO cold phase and only phosphate is available with a minor increase (Table 1).

In the global PDO distribution (Suppl. Fig. S1, top) the Oyashio region in the western North Pacific is located in a reversed temperature anomaly pattern compared to the eastern Pacific, so one might expect to see the opposite trends. The oxygen decreases during the cold PDO phase and slightly increases during the warm PDO phase. The nutrients increased during both PDO phases except for silicate which decreased during the cold PDO phase (Fig. 7, Table 1). Different to the other regions, the temperature of the 50 to 300 m layer shows a~~ significant~~ decrease in this region (Suppl. Fig. S2). The oxygen and nitrate of the Oyashio region show strong~~significant~~ correlations with the PDO (Table 2) with the PDO lagging by 4 to 5 years, indicating a delay between the surface signal and the changes in the subsurface layer. In a previous study where oxygen concentrations were investigated from 1954 to 2014, a decrease of oxygen was attributed to a reduction of ventilation in winter due to warming and freshening and reduction of dense water formation in the Sea of Okhotsk (Sasano et al., 2018).

At the 137°E region, except for nitrate with a negative trend during the cold PDO phase and a positive trend during the warm PDO phase oxygen increases and silicate and phosphate decrease during both phases (Suppl. Fig. S5). This indicates that there should be no strong correlation to the PDO phase, however the correlation reaches 0.45 ($p < 0.001$). According to the PDO expression on sea surface temperature (Suppl. Fig. S1) the PDO signal should be weak in the southwestern North Pacific. For the period 1985 to 2010 Takatani et al. (2012) described an oxygen decrease at the 137°E section, however during this time period also our oxygen measurements are quite similar and the posite oxygen trend is mainly caused by low oxygen values before 1970 and high oxygen values since 2010.

In the Peru region there is an increase in oxygen in the 50 to 300 m layer during the cold PDO phase and a decrease during the warm PDO phase. Nitrate, silicate and phosphate show trends opposite to oxygen. Despite the paucity of data in this region, these PDO related trends are within the 95% confidence limit for oxygen in the cold PDO phase, and for nitrate and phosphate since 1977 (Table 1).

The correlation of the PDO with the 50 to 350 m oxygen is ~~high (r=~~+0.~~6~~45 (p = 0.012)). This indicates that the observed changes in oxygen and nutrients off Peru are associated with the PDO.

Although the time period since the shift from negative to positive PDO in 2013 is short, ~~al~~most~~ all~~ areas examined here show higher 50 to 300 m oxygen concentrations than the trend line for the period since 1978 and lower nitrate and silicate concentrations tha~~e~~n the trend line since 1977, except for the Aloha and 137°E regions, the oxygen in 2017 in the Peru region, and the El Niño year 2015/16 and The Blob at area P.

Figure 1 shows a global mean temperature increase before 1945, a stagnant temperature trend during the PDO cool phase between 1945 and 1976 and a temperature increase after 1976 despite this period encompassing a PDO warm and cold phase. As the influence of the warm PDO phase 1977 to 1999 and the cold phase 1999 to 2014 is not related to major oxygen and nutrient trend changes, the increasing temperature seems to be a major component of setting the long-term oxygen trend in the Pacific Ocean.

3.3 The influence of the North Pacific Gyre Oscillation (NPGO)

As the NPGO is defined for a smaller region in the northeast Pacific than the PDO, its largest influence on oxygen and nutrients is expected to be in the North Pacific. The NPGO index shows higher variability than the PDO index (e. g. Fig. 4). Strong NPGO minima were present in the years 1967, 1980, 1994, 2006 and 2015 and maxima in the years 1961, 1976, 1988, 2000 and 2010.

In the area P, the correlation with NPGO is -0.28~~35~~ (p = 0.029) for oxygen in the 50 to 300 m layer for the period since 1977 with NPGO leading by 4 years; and +0.58~~61 (and significant)~~ (p < 0.001) for nitrate with NPGO lagging by one year (Table 2). The oxygen data are highly variable which might have led to the low correlation with the NPGO, however the nitrate correlation as well as a correlation of NPGO with temperature of -0.40~~65~~ (p = 0.001) show a strong relationship with the NPGO in this region.

Since 1980, the maxima and minima of the CalCOFIc time series of nitrate, phosphate and silicate (Fig. 5) often agree with the NPGO maxima and minima. The correlation between the 50-300 m annual mean and the NPGO annual mean is -0.35~~3~~ (p = 0.006) for oxygen (Fig. 6b) and +0.35~~8~~ (p = 0.025) for nitrate with the NPGO lagging by 1 year. The correlation with the NPGO is slightly weaker~~stronger~~ than with the PDO~~ in the North Pacific at area P and weaker~~ at CalCOFIc. This confirms the described decadal variations linked to the NPGO in the North Pacific and the California Current System (Di Lorenzo et al., 2009).

In the Oyashio region, oxygen shows a~~ significant~~ correlation of +0.35~~44~~ (p = 0.005) with the NPGO, and~~while~~ the correlation of nitrate and temperature with the NPGO are of similar strength~~weaker and not significant~~. In the western part of the North Pacific at 137°E the correlation with the NPGO is weak (-0.19; p = 0.163). At the southern part of the North Pacific subtropical gyre, in the Aloha area, the NPGO correlation coefficient of +0.39 (p = 0.008)~~56~~ with oxygen is~~ high and large~~ similar to~~r than~~ the PDO correlation. In the central equatorial Pacific and off Peru the correlation of oxygen with NPGO is ~~significant but~~ lower than the correlation with the PDO.

3.4 The influence of ~~the Sub-Tropical Cells (STC),~~ the North Pacific Index (NPI) and El Niño-Southern Oscillation (ENSO)

~~The strongest influence of the STC is expected in the tropical Pacific. For negative PDO phases tropical-extratropical interactions should lead to reduced mass flux in the STC and a reduction in the eastward flowing Equatorial Undercurrent (Henley, 2017). The reduced STC water transport from the 1960s to the 1990s should lead to reduced oxygen and nutrient transports to the tropics. After this, increased STC should lead to increased oxygen and nutrient transports in the early 2000s. Duteil et al. (2014) state that the simulated decrease in strength of the STC of about 30% during the 1960s to 1990s is in good agreement with observations and should induce a decline in tropical ocean oxygen and phosphate concentrations and a pause in oxygen decrease in the near future. The oxygen concentration at 50 to 300 m decreases at the equator at 165° to 175°W (area E) and 105° to 115°W (area D) over the entire record (1950-2017), while at 2° to 5°S, 84° to 87°W (area G) oxygen increases until the late 1970s and then decreases until 2017 (Fig. 3 and 4). However, at 165° to 175°W (area E), and 84° to 87°W (area G) the oxygen concentration increases after 2000 and this might be a signal related to the STC. The changes of the trend in oxygen and nutrients in the late 1970s in the eastern equatorial region (Fig. 3 and 4) suggest that these trends are not well correlated to STC changes. Due to the long duration~~

~~of the STC phases and the sparse data set, it is not possible to perform a meaningful correlation analysis to investigate STC influence on the oxygen and nutrient variations.~~

The bi-decadal oscillation related to NPI with minima in 1962 and 1983 and maxima in 1971 and 1991 (Watanabe et al., 2003, their Fig. 2) is difficult to see in our analysis of the Oyashio region due to large year-to-year variability (Fig. 7). The correlation of the NPI (November to March anomaly) with the 50 to 300 m oxygen time series in the North Pacific ~~since 1977~~ leads to ~~significant~~ correlations of 0.38 (p = 0.002)~~of -0.30~~ at the Oyashio region~~, and~~ 0.37 (p = 0.002) at area P, -0.42 (p= 0.002) at CalCOFIc, 0.33 (p = 0.025) at Aloha and -0.29 (p = 0.029) at 137°E~~44 at area P, without a time lag at either locations~~.

A bidecadal oscillation of 16.4-19.6 years in oxygen, possibly driven by nodal tidal cycles of 18.6 years, was described recently for the Oyashio region with maxima at about 1971, 1989 and 2008 and minima at about 1962, 1980 and 1998 (Fig. 3 in Sasano et al., 2018). The 50 to 300 m oxygen time series does not show a strong visual correlation for the period 1961 to 2008 between the trend-corrected oxygen and an 18.6 year oscillation. At area P oxygen trends include periods of increased ventilation of deeper isopycnals on a ~18 year cycle (Whitney et al., 2007). The correlation of the~~detrended~~ oxygen content of the 50 to 300 m layer ~~for the period 1954 to 2017~~ with a 18.6 year cycle for the Oyashio region was ~~significant with r = -0.27~~ 0.14 (p = 0.244). The correlation with the 18.6 year oscillation is 0.084 (p = 0.51)~~similar (0.25)~~ at area P, -0.139 (p = 0.28)~~but is weak and not significant~~ at~~both the~~ CalCOFIc~~, and~~ 0.146 (p = 0.339) at~~the~~ Aloha and -0.142 (p = 0.287) at 137°E~~areas~~. Although the 18.6-year tidal cycle could play a role as a basic forcing for the bi-decadal ocean variations (Yasuda et al. 2006) the correlation in the North Pacific is much stronger with the NPI than with the 18.6-year oscillation, likely due to short-term fluctuations in the NPI and the observed data or the sensitivity to phase shifts in the oscillation.

Similar parameter distributions as for cold PDO periods exist for La Niña events and as for warm PDO periods for El Niño events (Deutsch et al., 2011). Surprisingly in the equatorial regions (Fig. 3 and 4) the subsurface oxygen concentration at 50 to 300 m depth shows no clear anomalies in years of ENSO events. The ENSO signal seems to be restricted to the near surface layer in the equatorial Pacific. In the eastern Pacific during El Niño periods, oxygen in the upper ocean is higher and nutrients are lower in the upwelling regions (CalCOFIc and Peru region) due to either reduced upwelling or upwelling of oxygen-richer and nutrient poorer water masses. In the CalCOFIc region, the measurements during the very strong El Niño events in 1997/98 and 2015/16 show higher oxygen concentration and very low nutrient concentration in the 50 to 300 m layer when compared to the trend-line and the neighbouring years (Fig. 5). The deviations are very strong for the 1997/98 El Niño while moderate for the 2015/2016 El Niño. This signal is also visible for the 2015/2016 El Niño in the Peru region (Suppl. Fig. S6~~5~~) and for the 1997/98 El Niño at a shelf station off Lima (Graco et al., 2017). Not all strong El Niño events are associated with similar anomalies. Offshore from the upwelling region, at area P, the anomalies for the very strong El Niños 1997/98 and 2015/2016 are opposite, with low oxygen and high nutrient concentrations during the earlier event (Suppl. Fig. S3). For La Niña events a reversed trend is visible in the eastern Pacific for some events, e.g. with low oxygen and high nutrient concentrations for the 1988/1989, the 1998/1999 and the 1999/2000 La Niña events in the CalCOFIc region (Fig. 5). These ENSO related signals disappear in the following year and hence the ENSO related changes in oxygen and nutrients do not show a multi-year signal.

4 Discussion

One might wonder if the observed changes in trends in oxygen and nutrients are ~~more strongly~~ influenced by evolving methods rather than changes in climate. While the Winkler titration method to measure oxygen has remained the same since the early 1900’s, the methods to determine nutrients have varied over time. However, except for the very low nutrient data in the Aloha region in the center of the North Pacific, all areas ~~used~~ analyzed here show a similar and relatively large range for nitrate, silicate and phosphate. Precision of 5% for nitrate measurements of more than 10 µmol L^{-1}, of about 6% or less for silicate and 5% for phosphate at 0.9 µmol L^{-1} and larger are reported for early nutrient measurements (Hansen and Koroleff, 1999). Similar offsets for measurements after the 1990’s were derived with 3.5% for nitrate, 6.2% for silicate and 5.1% for phosphate (Tanhua et al., 2010), accordingly the offsets for the eastern equatorial region (Fig. 4) could be as high as ~1 µmol kg^{-1} for nitrate, ~0.1 µmol kg^{-1} for phosphate and ~1.0 µmol kg^{-1} for silicate and hence smaller than the observed long-term trends.

To put the regions examined here in context, we compare with previously published trends for the entire North Pacific as well as changes ~~influencing~~ with impact on the ocean circulation. Yasunaka et al. (2016) reported trends of surface phosphate and silicate averaged over the North Pacific from 1961 to 2012 as -0.012 ± 0.005 µmol l^{-1} $decade^{-1}$ and -0.38 ± 0.13 µmol l^{-1} $decade^{-1}$, respectively, whereas the nitrate trend averaged over the North Pacific was 0.01 ± 0.13 µmol l^{-1} $decade^{-1}$. This is in contrast to the subsurface layer examined here, where nitrate tended to increase over a similar time period. In particular, high nitrate increase was observed for the Oyashio region with +0.143 µmol kg^{-1} yr^{-1} for the period 1977 to 2017 (Table 1). An increase in anthropogenic nitrogen emissions from northeastern Asia and subsequent deposition over the North Pacific resulted in a detectable increase of nitrate concentrations in the near surface layer since the 1970s (Kim et al., 2014). The observed nitrate increase at 50 to 300 m might be the response of decreased water subduction. For example, the North Pacific Intermediate Water is a dominant pathway to enter the mid depth waters in the North Pacific and was freshening in the period 1960 to 1990 (Wong et al., 2001). Since the overturning in the North Pacific originates from the Okhotsk Sea through dense shelf water the observed freshening to depth of ~500 m during the past four decades could possibly weaken the shallow overturning of the North Pacific (Ohshima et al., 2014). Thus ~~interior~~ overturning ocean circulation in the North Pacific is likely slowing because less dense water is forming in the Sea of Okhotsk (Sasano et al., 2015, 2018) and hence decreasing the supply of oxygen.

Model results indicate that more than 50% of the total internal variability of oxygen is linked to the PDO in the North Pacific surface and subsurface waters (Frölicher et al., 2009). The long-term 50-300 m trends since the 1950s in the eastern equatorial Pacific and the CalCOFIc region (Fig. 4 and 5; Table 1) indicates a long-term increase in nitrate and phosphate and a decrease in silicate, but often with reversed trends in oxygen and nutrients when separated into cold and warm PDO phases. From the 1980s to the 2010s in the North Pacific, oxygen decreased while nitrate, phosphate and silicate increased (Whitney et al., 2013), similar to what was observed in the eastern equatorial Pacific and the CalCOFIc region for the period after 1976 (Fig. 4 and 5). For the California Current system the decadal oxygen changes seem to be primarily controlled by ocean circulation dynamics (Pozo Buil and Di Lorenzo, 2017). Pozo Buil and Di Lorenzo (2017) found that subsurface anomalies in the core of the North Pacific Current propagate the oxygen signal downstream within about 10 years to the coastal regions, and predicted a strong decline in oxygen by 2020 in the California Current system. The recent measurements in the CalCOFIc region, shown here, support this prediction.

The nutrient increase in the CalCOFIc region since the 1980s could be related to upwelling variability in the California Current. A strong nitrate flux from 1980 to 2010 was driven almost entirely by enhanced equatorward winds, negating a weak negative trend associated with increased surface heat flux (Jacox et al., 2015). However, changes in the properties of source waters (primarily from the eastern tropical Pacific via the California Undercurrent) have likely driven most of the biogeochemical trends observed in the southern California Current (Meinvielle and Johnson, 2013; Bograd et al., 2015; Nam et al., 2015).

Despite the low data coverage, the measurements in the Peru region confirm the expected opposite trends for oxygen and nutrients related to the PDO-phases. For a shallow shelf station (145 m depth) near Lima, measurements in the upper 100 m show increasing oxygen concentrations for the period 1999 to 2011 (Graco et al., 2017). This contrasts with the decreasing oxygen trend we observe from 1977 to 2017 in the Peru region (Suppl. Fig. S6~~5~~, Table 1) and indicates that different processes and trends might exist on the shelf compared to the open ocean.

~~In the equatorial Pacific time series no clear signal of the STC on oxygen and nutrients was observed.~~ In the eastern tropical and subtropical Pacific very strong El Niño and some strong La Niña events are apparent in the oxygen and nutrient distribution but do not result in a multi-year signal or trend.

5 Concluding remarks

In this study, we investigated the influence of well-documented atmosphere-ocean decadal oscillations on the trends in oxygen and nutrients in the upper subsurface layer of the Pacific Ocean. Due to the limited subsurface nutrient data, only select areas ~~could be~~were investigated and the results ~~might~~may have larger uncertainties for the areas with low data coverage and in particular for the combination of the warm and cold PDO periods after 1976. Especially in the South Pacific data are sparse, in part because not all existing data have been made public. A test excluding the winter months (January to March) in the area P and the Oyashio region (Supplementary Table S1) showed that the seasonal cycle had little influence on the trends derived for the 50 to 300 m layer. The depth layer of 50 to 300 m was selected as this is the major layer of biological subsurface activity influenced by oxygen and nutrient variability. For example, several warm-water mesopelagic species in the California Current, which are apparently adapted to the shallower, more intense OMZ off Baja California, were shown to be increasing despite declining midwater oxygen concentrations and becoming increasingly dominant (Koslow et al., 2018). Enhanced biological activity in coastal regions might lead to larger nutrient variability and obscure climate related signals. One also has to keep in mind that ~~As the layer investigated is subsurface, t~~the results might be influenced to a degree by changes in the propagation of water masses, as the ocean dynamics are non stationary.

Agreeing well with the regions with the largest SST signal of the PDO (Suppl. Fig. S1a), the PDO seems to have the strongest influence in the 50 to 300 m layer in the equatorial and eastern Pacific (Table 2). During the cold PDO phase in the eastern Pacific and the stagnant global surface temperature signal, the CalCOFIc region and the Peru region the 50 to 300 m oxygen increases and the nutrient concentrations decrease (Fig. 5, Suppl. Fig. S6~~5~~) and show the opposite trends during the global warming period since 1977, which we call the warm PDO phase despite a period of a PDO cool phase (Figure 1). An increase of oxygen from 1950 to 1980 and a decrease after 1980 has also been described for some isopycnal surfaces in subsurface waters of the Northeast Pacific (Crawford and Peña, 2016). In the western Pacific at 137°E the influence of the PDO should be weak and even a long-term oxygen increase was observed despite a large correlation coefficient with the PDO.

With respect to other climate indices, the results are more mixed. The NPGO has the largest impact on decadal variations in the North Pacific at area P (Table 2). The NPGO influence is also visible in the central and eastern North Pacific and the equatorial Pacific, although weaker than the correlation with the PDO. The NPI is well correlated to the oxygen changes in the North Pacific with the largest correlation at CalCOFIc~~Oyashio region and area P, without a time lag at either location~~. The 18.6 year nodal tidal cycle has the largest correlation in the Oyashio region,~~ and~~ the area P and CalCOFIc, however the correlation is weak compared to the correlation with the NPI.~~ but is not visible in the CalCOFIc and the Aloha regions.~~ In the Oyashio region a combination of the PDO, the NPGO, the NPI and the 18.6 year nodal cycle contributes to the trends in temperature, oxygen and nitrate. The oxygen decline in the Oyashio region has different controlling mechanisms for different depth layers. In the upper layer above σ_θ=26.7 kg m^{-3} (~200 m) the oxygen decline is primarily attributed to the reduction of winter convection upstream and in part to the deepening of isopycnal surfaces due to warming and freshening in the upper layers, while below σ_θ=26.7 kg m^{-3} the oxygen decline is attributed to the reduction of Dense Shelf Water formation in the Sea of Okhotsk associated with the reduction of sea ice production and freshening (Sasano et al., 2018).

The PDO and NPGO strongly influence the trends in oxygen and nutrient inventories; nevertheless the long-term sea surface temperature trend (Fig. 1) seems to play a role in the oxygen trend as long-term trends indicate an oxygen decrease throughout the cold and warm PDO phases in all but two~~one~~ areas. Note that while the most likely basin-wide drivers of oxygen and nutrient variability were investigated here, other contributors might exist depending on the region, as shown in detail for the Oyashio region by Sasano et al. (2018).

As greenhouse gas concentrations rise further, a variable but positive trend of increasing global mean surface temperature is expected, which should lead to a continuing decrease of oxygen and increase of nutrients in the subsurface layer important for biological activity. These biogeochemical changes can be expected to have significant economic consequences through changes in the availability of living marine resources.

Data availability

The NPGO Time series was taken from Emanuele Di Lorenzo, Georgia Tech http:www.o3d.org/npgo/npgo.php on 14~~8~~ August~~September~~ 2019~~8~~ with data available for January 1950 to July~~February~~ 2019~~8~~. The yearly PDO data were taken from http://ds.data.jma.go.jp/tcc/tcc/products/elnino/decadal/annpdo.txt on 18 September 2018 from the

Japan Meteorological Society covering the period 1901 to 2017. The NPI November to March anomaly was downloaded from NCAR climate data set https://climatedataguide.ucar.edu/climate-data/north-pacific-np-index-trenberth-and-hurrell-monthly-and-winter (status 4 January 2019, covering the period 1900 to 2018). The historical hydrographic data sets used here are as in Schmidtko et al. (2017), the references are listed in their paper in the Extended Data Table 2). The bottle data from cruises in 2016 at 170°W (096U2016426_hyd1.csv) and at 110°W (33RO20161119_hyd1.csv) were downloaded from the CCHDO at the University of California San Diego https://cchdo.ucsd.edu on 8 November 2018).

The CalCOFI data set downloaded from the California Cooperative Oceanic Fisheries Investigations http://www.calcofi.org/ccdata.html, status 13 August 2018; data period March 1949 to November 2017. Station P data (at 50°N, 145°W) are from the Institute of Ocean Sciences, Sidney BC, Canada (status September 2018) for the time period May 1956 to August 2017.

The Oyashio region data are from hydrodata, and updated data collections used in Whitney et al. (2013) and Sasano et al. (2018). The Aloha station data (at 22°45'N, 158°W were downloaded from the University of Hawaii web-page http://hahana.soest.hawaii.edu/hot/hot-dogs/bextraction.html status 15 January 2019, time period covered October 1988 to December 2017).

The assembled measurements of the Meteor cruises in February 2009, November 2012, December 2012, March 2017 and June 2017 and the Sonne cruise in October 2015 and the 137°E data added for 2008 to 2018 used in this paper will be made available before final publication.

A Supplement is related to this article.

Author contributions. L. Stramma conceived the study, wrote the manuscript had been chief scientist on two of the RV *Meteor* cruises and carried out the hydrographic measurements on two other Pacific cruises. S. Schmidtko handled the large-scale data sets and developed the optimal interpolation. T. Ono and D. Sasano provided the expertise and data for the Oyashio region, D. Sasano provided also data for the 137°E section, F. Whitney and T. Ross the data set and expertise for the North Pacific and S. Bograd his expertise for the CalCOFI region. All authors discussed and modified the manuscript.

Competing interests. The authors declare that they have no conflict of interest.

Acknowledgements. The Deutsche Forschungsgemeinschaft (DFG) provided support as part of the "Sonderforschungsbereich 754: Climate-Biogeochemistry Interactions in the Tropical Ocean" and for the RV *Meteor* cruises. We thank M. Robert and Fisheries and Oceans Canada staff for the core measurements on Line P cruises, as well as the innumerable scientists and crew who have contributed to the Line P program since 1956. The Line P ocean monitoring program is funded by Fisheries and Oceans Canada.

We are grateful to Miriam O'Brien who prepared the figure for http://blog.hotwhopper.com/ and her permission to use the figure in this publication.

References

Amrhein, V., Greenland, S. and McShane, B.: Retire statistical significance, Nature, 567, 305-307, 2019.

Bograd, S. J., Pozo Buil, M., Di Lorenzo, E., Castro, C. G., Schroeder, I. D., Goericke, R., Anderson, C. R., Benitez-Nelson, C., Whitney, F. A.: Changes in source waters to the Southern California Bight, Deep-Sea Res. II, 112, 42-52, https://doi.org/10.1016/j.dsr2.2014.04.009, 2015.

Bond, N.A., Cronin, M.F., Freeland, H. and Mantua, N.: Causes and impacts of the 2014 warm anomaly in the NE Pacific, Geophys. Res. Lett., 42, 3414-3420, https://doi.org/10.1002/2015GL063306, 2015.

Bretherton, F. P., Davis, R. E., and Fandry, C. B.: A technique for objective analysis and design of oceanographic experiments applied to MODE-73, Deep-Sea Res., 23, 559-582, https://doi.org/10.1016/0011-7471(76)90001-2, 1976.

Chavez, F. P., Ryan, J., Lluch-Cota, S. E., and Ňiquen, M.: From Anchovies to Sardines and back: Multidecdal change in the Pacific Ocean, Science, 299, 217, doi: 10.1126/science.1075880, 2003.

Crawford, W. R., and Peña, M. A.: Decadal trends in oxygen concentration in subsurface waters of the Northeast Pacific Ocean, Atmosphere-Ocean, 54, 171-192, 2016.

Czeschel, R., Stramma, L., Schwarzkopf, F. U., Giese, B. J., Funk, A., and Karstensen, J.: Middepth circulation of the eastern tropical South Pacific and its link to the oxygen minimum zone, J. Geophys. Res., 116, C01015, https://doi.org/10.1029/2010JC006565, 2011.

Czeschel, R., Stramma, L., and Johnson, G. C.: Oxygen decreases and variability in the eastern equatorial Pacific, J. Geophys. Res., 117, C11019, https://doi.org/10.1029/2012JC008043, 2012.

Czeschel, R., Stramma, L., Weller, R. A., and Fischer, T.: Circulation, eddies, oxygen and nutrient changes in the eastern tropical South Pacific, Ocean Sci., 11, 455-470, https://doi.org/10.5194/os-11-455, 2015.

Deser, C., Alexander, M. A., Xie, S.-P., and Phillips, A. S.: Sea surface temperature variability: Patterns and mechanisms, Annu. Rev. Mar. Sci., 2, https://doi.org/10.1146/annurev-marine-120408-151453, 2010.

Deutsch, C., Brix, H., Ito, T., Frenzel, H., and Thompson, L.: Climate-forced variability of ocean hypoxia, Science, 333, 336-339, https://doi.org/10.1126/science.1202422, 2011.

Di Lorenzo, E., Mantua, N. J.: Multi-year persistence of the 2014/15 North Pacific marine heat wave. Nature Climate Change, 6(11), 1042-1047, https://doi.org/10.1038/nclimate3082, 2016.

Di Lorenzo, E., Schneider, N., Cobb, K. M., Franks, P. J. S., Chhak, K., Miller, A. J., McWilliams, J. C., Bograd, S. J., Arango, H., Curchitser, E., Powell, T. M., and Riviere, P.: North Pacific Gyre Oscillation links ocean climate and ecosystem change, Geophys. Res. Lett., 35, L08607, https://doi.org/10.1029/2007GL032838, 2008.

Di Lorenzo, E., Fiechter, J., Schneider, N., Bracco, A., Miller, A. J., Franks, P. J. S., Bograd, S. J., Moore, A. M., Thomas, A. C., Crawford, W., Peña, A., and Hermann, A. J.: Nutrient and salinity decadal variations in the central and eastern North Pacific, Geophys. Res. Lett., 36, L14601, https://doi.org/10.1029/2009GL038261, 2009.

~~Duteil, O., Böning, C. W., and Oschlies, A.: Variability in subtropical-tropical cells drives oxygen levels in the tropical Pacific Ocean, Geophys. Res. Lett., 41, https://doi.org/10.1002/2014GL061774, 2014.~~

Duteil, O., Oschlies, A., and Böning, C. W.: Pacific Decadal Oscillation and recent oxygen decline in the eastern tropical Pacific Ocean, Biogeosciences, https://doi.org/10.5194/bg-15-7111-2018, 2018.

Frölicher, T. L., Joos, F., Plattner, G.-K., Steinacher, M., and Doney, S. C.: Natural variability and anthropogenic trends in oceanic oxygen in a coupled carbon cycle-climate model ensemble, Global Biogeochemical Cycles, 23, https://doi.org/10.1029/2008GB003316, 2009.

Graco, M. I., Purca, S., Dewitte, B., Castro, C. G., Morón, O., Ledesma, J., Flores, G., and Gutiérrez, D.: The OMZ and nutrient features as a signature of interannual and low frequency variability off the Peruvian upwelling system, Biogeosciences, 14, 4601-4617, https://doi.org/10.5194/bg-14-4601-2017, 2017.

Hansen, H. P.: Determination of oxygen. In: Methods of Seawater analysis, edited by: Grasshoff, K., Kremling, K., and Ehrhardt, M., Wiley-VCH, Weinheim, Germany, 75-89, 1999.

Hansen, H. P., and Koroleff, F.: Determination of nutrients. In: Methods of Seawater analysis, edited by: Grasshoff, K., Kremling, K., and Ehrhardt, M., Wiley-VCH, Weinheim, Germany, 149-158, 1999.

Hansen, J., Ruedy, R., Sato, M., and Lo, K.: Global surface temperature change, Rev. Geophys., 48, RG4004, https://doi.org/10.1029/2010RG000345, 2010.

~~Henley, B. J.: Pacific decadal climate variability: Indices, patterns and tropical-extratropical interactions, Global and Plenetary Change, 155, 42-55, https://doi.org/10.1016/j.gloplacha.2017.06.004, 2017.~~

~~Hong, L., Zhang, L., Chen, Z., and Wu, L.: Linkage between the Pacific Decadal Oscillation and the low frequency variability of the Pacific Subtropical Cell, J. Geophys. Res. Oceans, 119, 3464-3477, https://doi.org/10.1002/2013JC009650, 2014.~~

IPCC: Climate Change 2013: The Physical Science Basis. Contribution of Working Group I to the Fifth Assessment Report of the Intergovernmental Panel on Climate Change. Stocker, T. F., Qin, D., Plattner, G.-K., Tignor, M., Allen, S. K., Boschung, J., Nauels, A., Xia, Y, Bex, V., and Midgley, P. M. (eds.). Cambridge University Press, Cambridge, United Kingdom and New York, NY, USA, 1535 pp, 2013.

Jackson, J. M., Johnson, G. C., Dosser, H. V., and Ross, T.: Warming from recent marine heatwave lingers in deep British Columbia Fjord, Geophys. Res. Lett., 45, 9757-9764, https://doi.org/10.1029/2018GL078971, 2018.

Jacox, M. G., Bograd, S. J., Hazen, E. L., and Fiechter, J.: Sensitivity of the California Current nutrient supply to wind, heat, and remote ocean forcing, Geophys. Res. Lett., 42, https://doi.org/10.1002/2015GL065147, 2015.

Kalvelage, T., Lavik, G., Lam, P., Contreras, S., Arteaga, L., Löscher, C. R., Oschlies, A., Paulmier, A., Stramma, L., and Kuypers, M. M. M.: Nitrogen cycling driven by organic matter export in the South Pacific oxygen minimum zone, Nature Geoscience, 6, 228-234, https://doi.org/10.1038/NGEO1739, 2013.

Karstensen, J., Stramma, L., and Visbeck, M.: Oxygen minimum zones in the eastern tropical Atlantic and Pacific oceans, Prog. Oceanogr., 77, 331-350, 2008.

Kessler, W.: The circulation of the eastern tropical Pacific: A review, Prog. Oceanogr., 69, 181-217, 2006.

Kim, I.-N., Lee, K., Gruber, N., Karl, D. M., Bullister, J. L., Yang, S., and Kim, T.-W.: Increasing anthropogenic nitrogen in the North Pacific Ocean, Science, 346, 1102-1106, 2014.

Koslow, J. A., Davison, P., Ferrer, E., Jiménez Rosenberg, S. P. A., Aceves-Medina, G., and Watson, W.: The evolving response of mesopelagic fishes to declining midwater oxygen concentrations in the southern and central California Current, ICES Journal of Marine Science, https://doi.org/10.1093/icesjms/fsy154, 2018.

Mantua, N. J, Hare, S. R., Zhang, Y., Wallace, J. M., and Francis, R. C.: A Pacific interdecadal climate oscillation with impacts on salmon production, Bull. Amer. Met. Soc., 78, 1069-1079, 1997.

~~McPhaden, M. J., and Zhang, D.: Slowdown of the meridional overturning circulation in the upper Pacific Ocean, Nature, 415, 603-608, 2002.~~

~~McPhaden, M. J., and Zhang, D.: Pacific Ocean circulation rebounds, Geophys. Res. Lett., 31, L18301, httpS://doi.org/10.1029/2004GL020727, 2004.~~

McPhaden, M. J., Zebiak, S. E., and Glantz, M. H.: ENSO as an Integrating Concept in Earth Science, Science, 314, 1740-1745, https://doi.org/10.1126/science.1132588, 2006.

McShane, B. B., Gal, D., Gelman, A., Robert, C., and Tacket, J. L.: Abandon Statistical Significance, The American Statistician, 73:sup1, 235-245, DOI: 10.1080/00031305.2018.1527253, 2019.

Meinvielle, M., and Johnson, G. C.: Decadal water-property trends in the California Undercurrent, with implications for ocean acidification, J. Geophys. Res. Oceans, 118, 6687-6703, https://doi.org/10.1002/2013JC009299, 2013.

Miller, A. J., Cayan, D. R., Barnett, T. P., Graham, N. E., and Oberhuber, J. M.: The 1976-77 climate shift of the Pacific Ocean, Oceanography, 7, 21-26, 1994.

Minobe, S.: Spatio-temporal structure of the pentadecadal variability over the North Pacific, Prog. Oceanogr., 47, 381-408, 2000.

Nam, S., Takeshita, Y., Frieder, C. A., Martz, T., and Ballard, J.: Seasonal advection of Pacific Equatorial Water alters oxygen and pH in the Southern California Bight, J. Geophys. Res. Oceans, 120, 5387-5399, https://doi.org/10.1002/2015JC010859, 2015.

Newman, M., Alexander, M. A., Ault, T. R., Cobb, K. M., Deser, C., Di Lorenzo, E., Mantua, N. J., Miller, A. J., Minobe, S., Nakamura, H., Schneider, N., Vimont, D. J., Phillips, A. S., Scott, J. D., and Smith, C. A.: The Pacific decadal oscillation, revisited, Journal of Climate, 29, 4399-4427, https://doi.org/10.1175/JCLI-D-15-0508.1, 2016.

Ohshima, K. I., Nakanowatari, T., Riser, S., Volkow, Y., and Wakatsuchi, M.: Freshening and dense shelf water reduction in the Okhotsk Sea linked with sea ice decline, Prog. Oceanogr., 126, 71-79, https://doi.org/10.1016/j.pocean.2014.04.020, 2014.

Oka, E., Ishii, M., Nakano, T., Suga, T., Kouketsu, S., Miyamoto, M., Nakano, H., Qiu, B., Sugimoto, S., and Takatani, Y.: Fifty yeara of the 137°E repeat hydrographic section in the western North Pacific Ocean,, Journal of Oceanography, 74, 115-145, https:/doi.org/10.1007/s10872-017-0461-x, 2018.

Ono, T., Shiomoto, A., and Saino, T.: Recent decrease of summer nutrients concentrations and future possible shrinkage of the subarctic North Pacific high-nutrient low-chlorophyll region, Global Biogeochemical Cycles, 22, GB3027, https://doi.org/10.1029/2007GB003092, 2008.

Oschlies, A., Brandt, P., Stramma, L., and Schmidtko, S.: Drivers and mechanisms of ocean deoxygenation, Nature Geoscience, 11, 467-473, https://doi.org/10.1038/s41561-018-0152-2, 2018.

Pozo Buil, M., and Di Lorenzo, E.: Decadal dynamics and predictability of oxygen and subsurface tracers in the California Current, Geophys. Res. Let., 44, https://doi.org/10.1002/2017GL072931, 2017.

Ridder, N. N., and England, M. H.: Sensitivity of ocean oxygenation to variations in tropical zonal wind stress magnitude, Global Biogeochemical Cycles, 28, 909-926, https://doi.org/10.1002/2013GB004708, 2014.

Royer, T. C.: High-latitude oceanic variability associated with the 18.6-year nodal tide, Journal of Geophysical Research, 98 C3, https://doi.org/10.1029/92JC02750, 1993.

Sasano, D., Takatani, Y., Kosugi, N., Nakano, T., Midorikawa, T., and Ishii, M.: Multidecadal trends of oxygen and their controlling factors in the western North Pacific, Global Biogeochemical Cycles, 29, 935-956, https://doi.org/10.1002/2014GB005065, 2015.

Sasano, D., Takatani, Y., Kosugi, N., Nakano, T., Midorikawa, T., and Ishii, M.: Decline and bidecadal oscillations of dissolved oxygen in the Oyashio Region and their propagation to the western North Pacific, Global Biogeochemical Cycles, 32, 909-931, https://doi.org/10.1029/2017GB005876, 2018.

Schmidtko, S., Johnson, G. C., and Lyman, J. M.: MIMOC: A global monthly isopycnal upper-ocean climatology with mixed layers, J. Geophys. Res. Oceans, 118, 1658-1672, https://doi.org/10.1002/jgrc.20122, 2013.

Schmidtko, S., Stramma, L., and Visbeck, M.: Decline in global oceanic oxygen content during the past five decades, Nature, 542, 335-339, https://doi.org/10.1038/nature21399, 2017.

Schott, F. A., Stramma, L., Wang, W., Giese B. S., and Zantopp, R.: Pacific subtropical cell variability in the SODA 2.0.2/3 assimilation, Geophys. Res. Lett., 35, L10607, https://doi.org/10.1029/2008GL033757, 2008.

Stramma, L., Johnson, G. C., Sprintall, J., and Mohrholz, V.: Expanding oxygen-minimum zones in the tropical oceans, Science, 320, 655-658, https://doi.org/10.1126/science.1153847, 2008.

Stramma, L., Schmidtko, S., Levin, L. A., and G. C. Johnson, G. C.: Ocean oxygen minima expansions and their biological impacts, Deep Sea Res., Part I, 57, 587–595, 2010.

Stramma, L., Bange, H. W., Czeschel, R., Lorenzo, A., and Frank M.: On the role of mesoscale eddies for the biological productivity and biogeochemistry in the eastern tropical Pacific off Peru, Biogeosciences, 10, 7293-7306, https://doi.org/10.5194/bg-10-7293-2013, 2013.

Stramma, L., Fischer, T., Grundle, D. S., Krahmann, G., Bange, H. W. and Marandino, C. A.: Observed El Niño conditions in the eastern tropical Pacific in October 2015, Ocean Sci., 12, 861-873, https://doi.org/10.5194/os-12-861-2016, 2016.

Takatani, Y., Sasano, D., Nakano, T., Midorikawa, T., and Ishii, M.: Decrease of dissolved oxygen after the mid-1980s in the western North Pacific subtropical gyre along the 137°E repeat section, Global Biogeochem. Cycles, 26, GB2013, doi:10.1029/2011GB004227, 2012.

Tanhua, T., van Heuven, S., Key. R. M., Velo, A., Olsen, A., and Schirnick, C.: Quality control procedures and methods of the CARINA database, Earth Syst. Sci. Data, 2. 35-49, 2010.

Trenberth, K. E.: Has there been a hiatus? Science, 349, 691-692, https://doi.org/10.1126/science.aac9225, 2015.

Ueno, H., and Yasuda, I.: Intermediate water circulation in the North Pacific subarctic and northern subtropical regions, J. Geophys. Res., 108, https://doi.org/10.1029/2002JC001372, 2003.

Wang, C., and Fiedler, P. C.: ENSO variability in the eastern tropical Pacific: A review, Prog. Oceanogr., 69, 239-266, 2006.

Watanabe, Y. W., Wakita, M., Maeda, N., Ono, T. and Gamo T.: Synchronous bidecadal periodic changes of oxygen, phosphate and temperature between the Japan Sea deep water and the North Pacific intermediate water, Geophys. Res. Lett, 30(24), 2273, https://doi.org/10.1029/2003GL018338, 2003.

Whitney, F. A., Freeland, H. J., and Robert, M.: Persistently declining oxygen levels in the interior waters of the eastern subarctic Pacific, Prog. Oceanogr., 75, 179-199, 2007.

Whitney, F. A., Bograd, S. J., and Ono, T.: Nutrient enrichment of the subarctic Pacific Ocean pycnocline, Geophys. Res. Lett., 40, 2200-2205, https://doi.org/10.1002/grl.50439, 2013.

Winkler, L. W.: Bestimmung des im Wasser gelösten Sauerstoffs, Ber. Dtsch. Chem. Ges., 21, 2843-2855, 1888.

Wong, A. P. S., Bindoff, N. L., and Church, J.A.: Freshwater and heat changes in the North and South Pacific Oceans between 1960s and 1985-94, Journal of Climate, 14, 1613-1633, 2001.

Yasuda, I., Osafune, S., and Tatebe, H.: Possible explanation linking 18.6-year period nodal tidal cycle with bi-decadal variations of ocean and climate in the North Pacific, Geophys. Res. Lett., 33, L08606, doi:10.1029/2005GL025237, 2006.

Yasunaka, S., Ono, T., Nojiri, Y., Whitney, F. A., Wada, C., Murata, A., Nakaoka, S., and Hosoda, S.: Long-term variability of surface nutrient concentrations in the North Pacific, Geophys. Res. Lett., 43, 3389-3397, https://doi.org/10.1002/2016GL068097, 2016.

Table 1. Linear trends of solutes in µmol kg^{-1} yr^{-1} with 95% confidence intervals (p-values) where data are available for the entire period since 1950, for negative (1950-1976; PDO-) and positive (after 1976; PDO+) PDO periods in the 50 to 300 m depth layer for selected ocean areas shown in Figures 3, 4, 5, 7, S3, S4, S5 and S6~~5~~. Trends whose~~not within the~~ 95% confidence interval includes zero are shown in *italics*. Areas named: CalCOFIc (34°-35°N, 121°-122°W), area P (48°-52°N, 143°-147°W), Aloha region (22°-25°N, 156°-159°W), Oyashio region (39°-42°N, 144°-149°E), 137°E (20°-26°N, 134°-140°E) and Peru region (7°-12°S, 78°-83°W).

Parameter	trend	time period	PDO- trend	time period	PDO+ trend	time period
Area E-	5°N-5°S, 165°-175°W		5°N-5°S, 165°-175°W		5°N-5°S, 165°-175°W	
Oxygen	-0.36 ± 0.22	1950-2016	*-0.19 ± 0.78*	1950-1975	*-0.56 ± 0.57*	1977-2016

Area D -	5°N-5°S, 105°-115°W	5°N-5°S, 105°-115°W	5°N-5°S, 105°-115°W
Oxygen	-0.65 ± 0.37 1957-2016	*-2.4* ± *3.1* 1957-1971	-0.84 ± 0.55 1979-2016
Area G-	2°-5°S, 84°-87°W	2°-5°S, 84°-87°W	2°-5°S, 84°-87°W
Oxygen	+*0.17* ± *0.48* 1955-2017	+1.63 ± 1.18 1955-1976	*-0.12* ± *0.54* 1979-2017
Nitrate	*-0.027*± *0.165* 1966-2017	*-0.594* ± *1.380* 1966-1976	+*0.065* ± *0.164* 1979-2017
Silicate	-0.079 ± 0.077 1960-2017	*-0.381* ± *0.545* 1960-1976	*-0.098* ± *0. 172* 1983-2017
Phosphate	+*0.003* ± *0.010* 1960-2017	*-0.018* ± *0.044* 1960-1976	+*0.011* ± *0.026* 1983-2017
Area	CalCOFIc	CalCOFIc	CalCOFIc
Oxygen	*-0.18* ± *0.41* 1950-2017	+1.13 ± 0.96 1950-1976	-0.58 ± 0.40 1978-2017
Nitrate	+*0.035* ± *0.054* 1969-2017	*-1.040* ± *4.230* 1969-1973	+0.066 ± 0.061 1978-2017
Silicate	*-0.021* ± *0.059* 1961-2017	*-0.215* ± *0.625* 1961-1973	+ *0.029* ± *0.091* 1978-2017
Phosphate	+*0.001* ± *0.003* 1950-2017	*-0.000* ± *0.016* 1950-1973	+0.006 ± 0.005 1978-2017
Area	area P	area P	area P
Oxygen	-0.24± 0.23 1954-2017	*-0.16* ± *1.41* 1954-1976	*-0.18* ± *0.42* 1977-2017
Nitrate	+0.071 ± 0.056 1956-2017	*-0.113* ± *0.515* 1956-1973	+*0.093* ± *0.096* 1980-2017
Silicate	+0.492 ± 0.180 1957-2017	+*1.47* ± *4.92* 1957-1971	+*0.193* ± *0.261* 1987-2017
Phosphate	+*0.001* ± *0.003* 1954-2017	*-0.013* ± *0.023* 1954-1971	+*0.001* ± *0.008* 1980-2017
Area	Aloha region	Aloha region	Aloha region
Oxygen	*-0.08* ± *0.21* 1951-2017	+*0.20* ± *0.45* 1951-1976	+*0.004* ± *0.38* 1977-2017
Nitrate	none	*none*	+*0.014* ± *0.021* 1984-2017
Silicate	+0.013 ± 0.013 1970-2017	none	+*0.013* ± *0.016* 1985-2017
Phosphate	-0.002 ± 0.001 1953-2017	+*0.007* ± *0.020* 1953-1966	*-0.0004* ± *0.002* 1985-2017

Area	Oyashio region	Oyashio region	Oyashio region
Oxygen	*-0.23 ± 0.34* 1952-2017	*-0.39 ± 0.60* 1952-1976	*+0.15 ± 0.69* 1977-2017
Nitrate	+0.090 ± 0.068 1964-2017	*+0.164 ± 0.520* 1964-1976	+0.143 ± 0.079 1977-2017
Silicate	*+0.176 ± 0.370* 1952-2017	-1.38 ± 1.09 1952-1972	+0.667 ± 0.330 1981-2017
Phosphate	+0.006 ± 0.004 1953-2017	*+0.010 ± 0.015* 1953-1976	+0.010 ± 0.007 1977-2017

Area	137°E	137°E	137°E
Oxygen	+0.06 ± 0.04 1955-2018	+0.25 ± 0.25 1955-1976	*+0.03 ± 0.07* 1977-2018
Nitrate	*-0.004 ± 0.011* 1966-2018	*-0.009 ± 0.126* 1966-1976	*+0.005 ± 0.008* 1977-2018
Silicate	-0.067 ± 0.028 1958-2018	*-0.068 ± 0.312* 1958-1970	-0.083 ± 0.066 1981-2018
Phosphate	-0.002 ± 0.001 1958-2018	*-0.005 ± 0.008* 1958-1976	*-0.001 ± 0.001* 1977-2018

Area	Peru region	Peru region	Peru region
Oxygen	*- 0.05 ±0.32* 1960-2017	+0.92 ± 0.68 1960-1976	*-0.34 ± 0.40* 1977-2017
Nitrate	*+0.068 ± 0.216* 1965-2017	*-1.03 ± 1.35* 1965-1976	+0.181 ± 0.073 1977-2017
Silicate	*-0.062 ± 0.150* 1965-2017	*-0.707 ± 1.040* 1965-1976	*+0.032 ± 0.145* 1977-2017
Phosphate	*-0.000 ± 0.010* 1960-2017	*-0.006 ± 0.032* 1960-1976	+0.012 ± 0.010 1977-2017

Table 2. Correlation coefficient and p-value for available data since 1950 between annual layer 50 to 300 m concentration and PDO and NPGO with PDO/NPGO lags (negative PDO/NPGO leads). Areas with large p-values >0.05 are considered not significant correlated.

Area	Parameter	PDO-lag	PDO-correlation(p)	NPGO-lag	NPGO-correlation(p)

5°N-5°S, 165°W-175°W	oxygen	-7	0.55 (0.001)	-7	-0.53 (0.002)
5°N-5°S, 105°W-115°W	oxygen	-1	0.71 (<0.001)	-3	-0.46 (0.055)
2°S-5°S, 84°W-87°W	oxygen	-11	0.83(<0.001)	-2	0.32(0.134)
CalCOFIc	oxygen	-11	0.42(0.002)	+1	-0.35(0.006)
CalCOFIc	nitrate	+1	-0.37(0.019)	+1	0.35(0.025)
Area P	oxygen	+10	-0.30(0.019)	-4	-0.28(0.029)
Area P	nitrate	+6	-0.27(0.109)	+1	0.58(<0.001)
Area P	temperature	+2	0.46(<0.001)	+1	-0.40(0.001)
Aloha region	oxygen	+2	-0.43(0.003)	+1	0.39(0.008)
Oyashio region	oxygen	+5	-0.50(<0.001)	-5	0.35(0.005)
Oyashio region	nitrate	+4	-0.27(0.049)	+7	0.37(0.006)
Oyashio region	temperature	+7	-0.44(<0.001)	+5	-0.27(0.032)
137°E	oxygen	+10	0.45(<0.001)	0	-0.19(0.163)
Peru region	oxygen	0	0.45(0.012)	+1	-0.26(0.155)

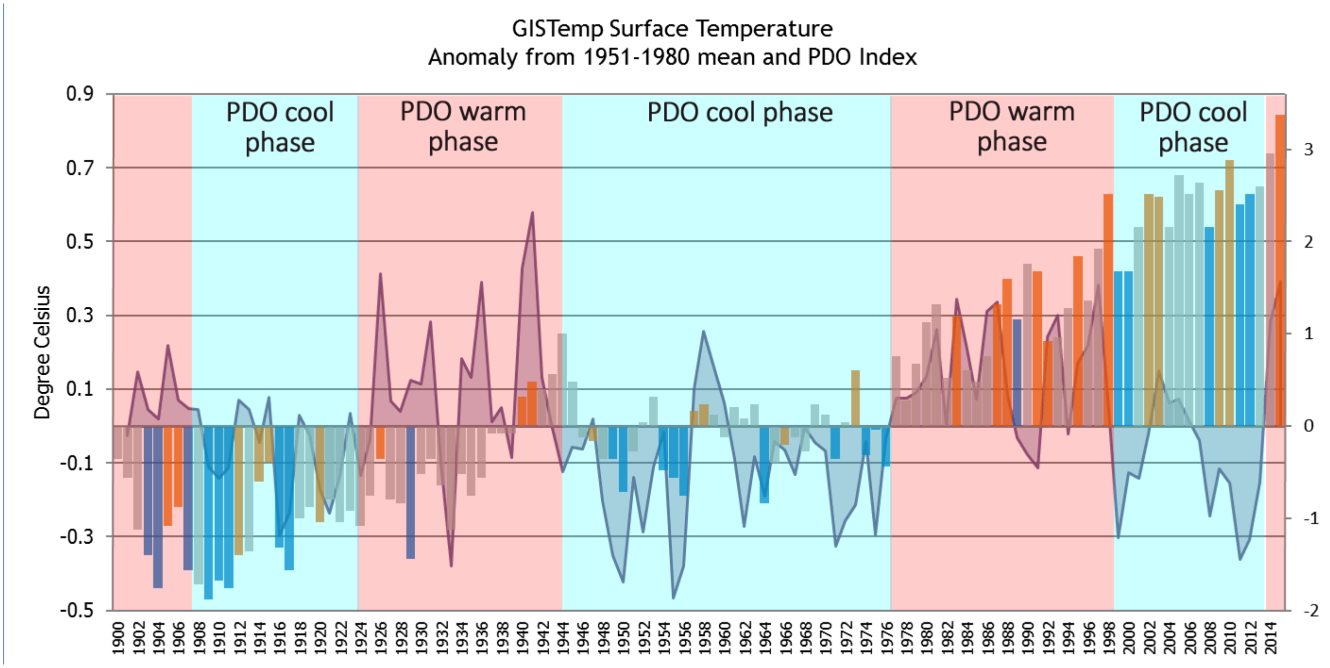

Figure 1. Global mean surface temperature anomaly from the 1951 to 1980 mean (GISTemp; peak of the annual bars; left scale) with La Niña years (blue bars), El Niño years (orange/brown bars) neutral years (grey bars) and the PDO index (solid line; right scale), with PDO phases marked (compiled by Miriam O'Brien for 1900 to 2015). The data sources used GISS NASA (temperature), Australian Bureau of Meteorology (ENSO years based on the Southern Oscillation Index) Japan Meteorological Society (PDO index) and Trenberth 2015 (PDO phases).

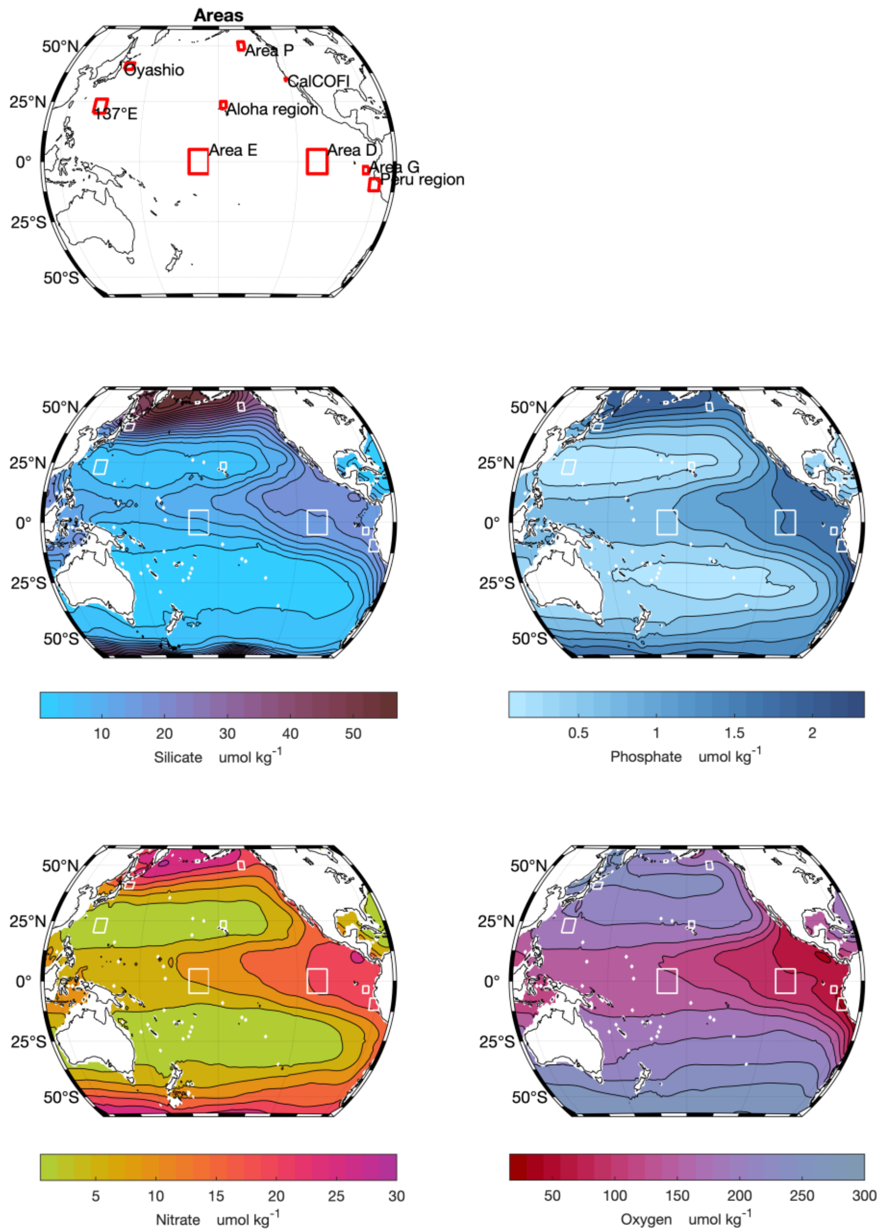

Figure 2. Distribution of the areas used and mean 50 to 300 m silicate, phosphate, nitrate and oxygen (all in µmol kg^{-1}), in the Pacific Ocean.

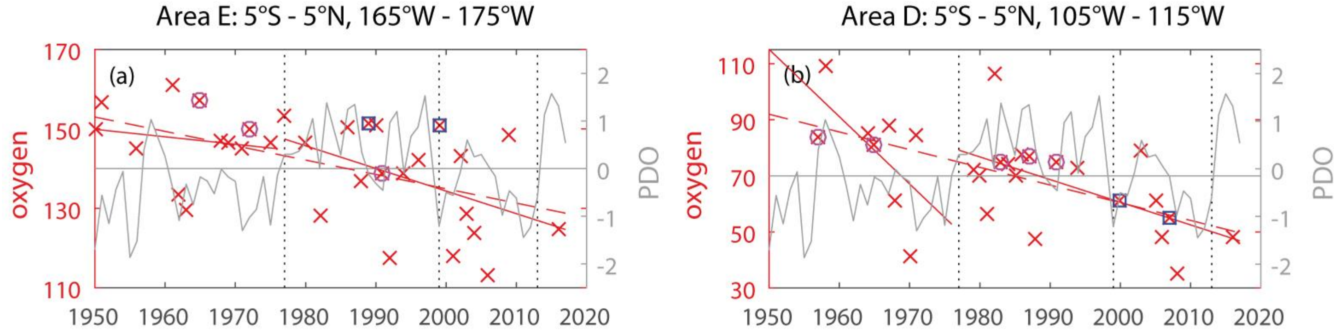

Figure 3. Annual mean oxygen concentration (in µmol kg^{-1}, red crosses) for years available and trends for the layer 50 to 300 m plotted for the entire time period (dashed red lines) and for the periods 1950 to 1976 for the negative PDO phase and after 1976 for the positive PDO phase (solid red lines) for a) 5°S-5°N, 165-175°W (area E) and b) 5°S-5°N, 105-115°W (area D). El Niño years defined as strong or very strong are marked by an additional magenta circle, strong La Niña years by an additional blue square. The change of the PDO status in 1977, 1999 and 2013 are marked by vertical dotted lines. The annual mean PDO index is shown as grey curve.

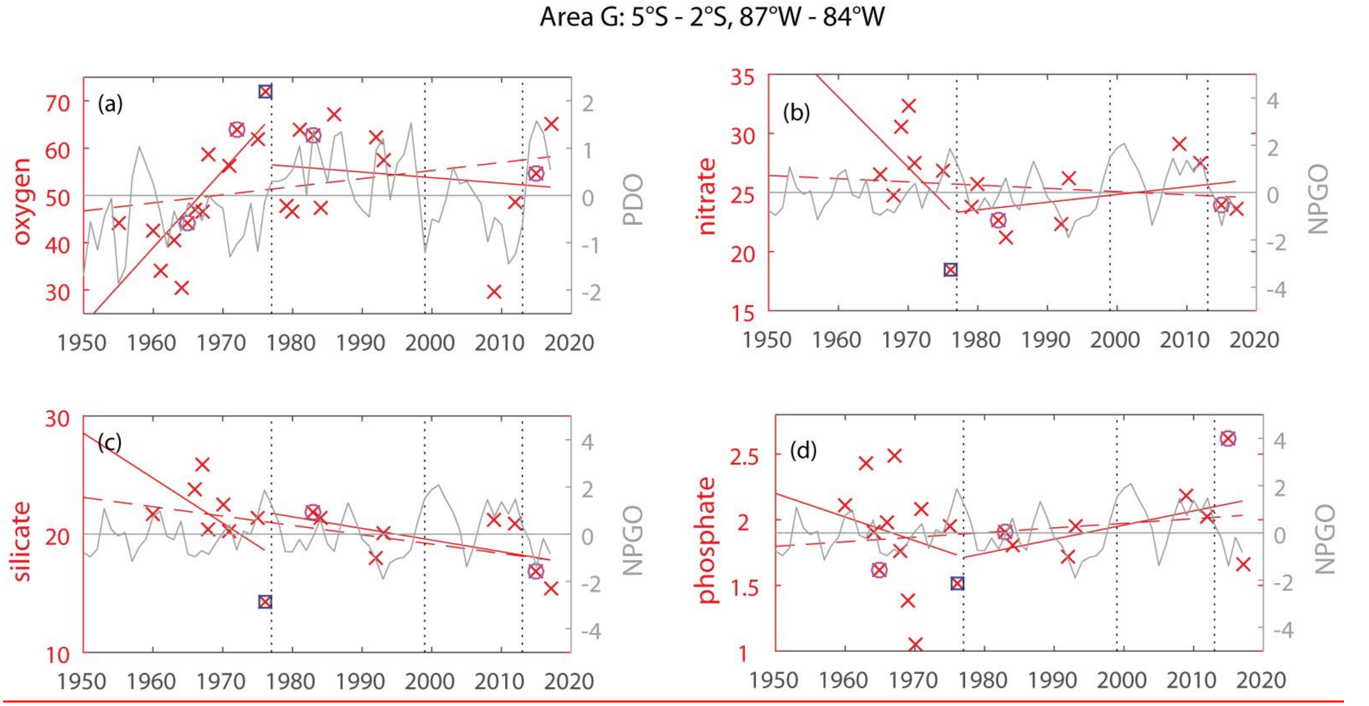

Figure 4. Annual mean concentration (in µmol kg^{-1}, red crosses) for years available (see Table 1) and trends for the layer 50 to 300 m plotted for the entire time period (dashed red lines) and for the periods 1950 to 1976 for the negative PDO phase and after 1976 for the positive PDO phase (solid red lines) between 2°S and 5°S, 84°W and 87°W (area G) in µmol kg^{-1} yr^{-1} for oxygen, nitrate, silicate and phosphate. El Niño years defined as strong or very strong are marked by an additional magenta circle, strong La Niña years by an additional blue square. For oxygen measurements in 1982 were removed as the 50-300 m mean was much too high 104.8 µmol kg^{-1}) and for nitrate measurements in 1967 which were too high (36.8 µmol kg^{-1}). The change of the PDO status in 1977, 1999 and 2013 are marked by vertical dotted lines. The annual mean PDO index is shown in the oxygen time series as grey curve and the NPGO index is shown in the nitrate, silicate and phosphate time series as grey curve.

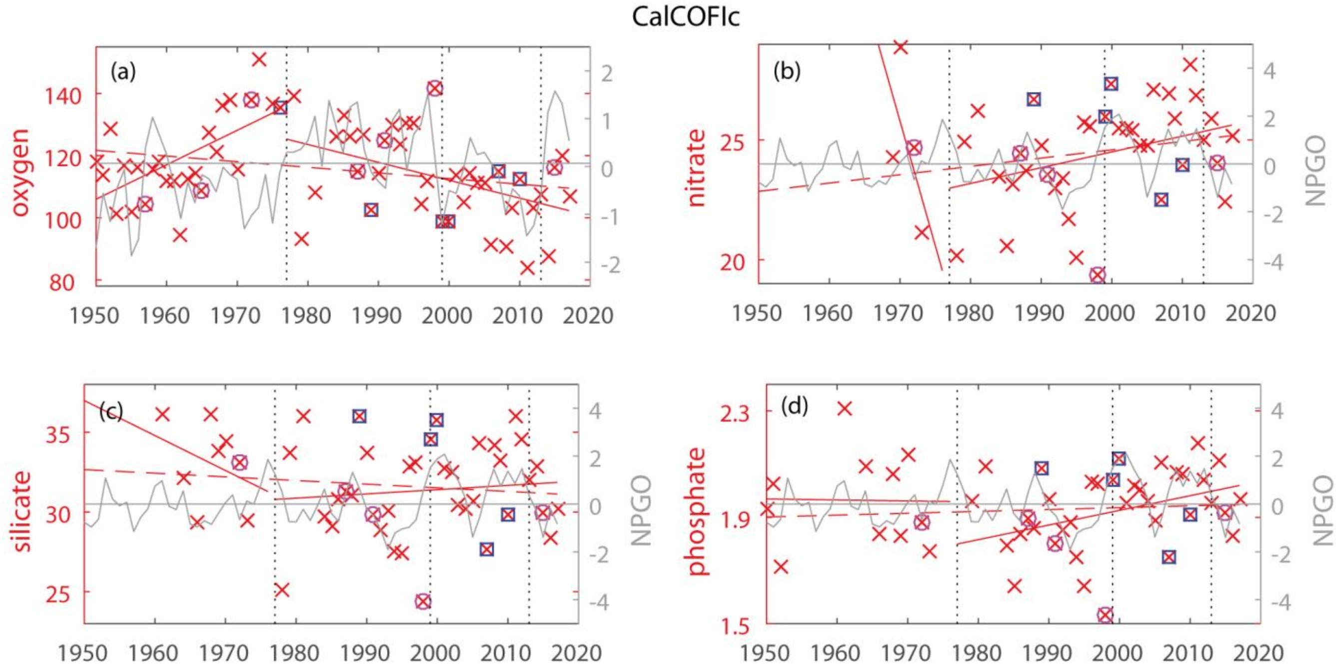

Figure 5. Annual mean concentration (in µmol kg^{-1}, red crosses) for years available and trends for the layer 50 to 300 m plotted for the entire time period (dashed red lines) and for the periods 1950 to 1976 for the negative PDO phase and after 1976 for the positive PDO phase (solid red lines) between 34°N and 35°N, 121°W and 122°W from the CalCOFIc bottle data in µmol kg^{-1} yr^{-1} for a) oxygen, b) nitrate, c) silicate and d) phosphate. El Niño years defined as strong and very strong are marked by an additional magenta circle, strong La Niña years by an additional blue square. The change of the PDO status in 1977, 1999 and 2013 are marked by vertical dotted lines. The annual mean PDO index is shown in the oxygen time series as grey curve and the NPGO index is shown in the nitrate, silicate and phosphate time series as grey curve.

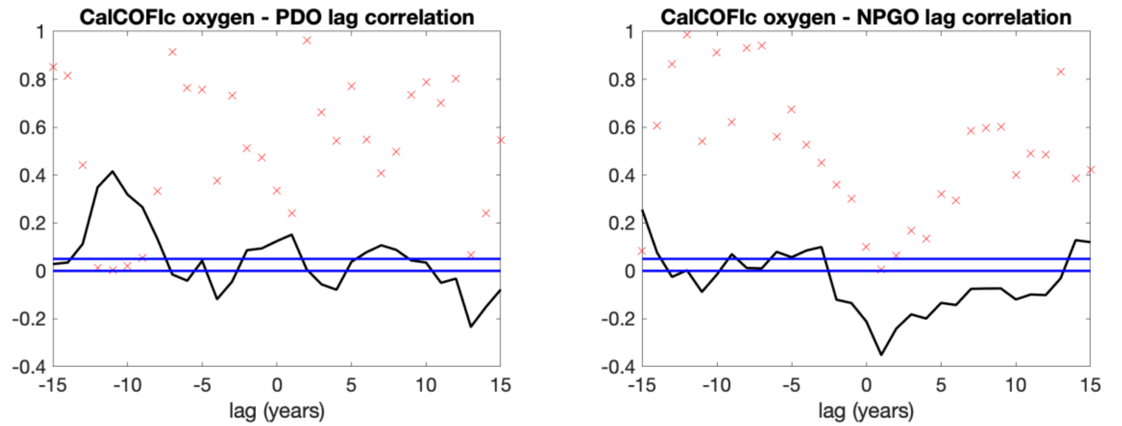

Figure 6. Correlation between oxygen at 50-300 m in the region 34-35°N, 121-122°W (CalCOFIc) and a) the PDO and b) the NPGO (black lines) shifted between -15 and +15 years for the years after 1976 ~~with the lower and upper bounds of the 95% confidence interval (red lines)~~ and the p-values (x) which ~~shows~~ often are used to declare non-significant correlation for p ~>0.05 (blue lines for 0 and 0.05). For positive years PDO/NPGO lags, for negative years they lead.

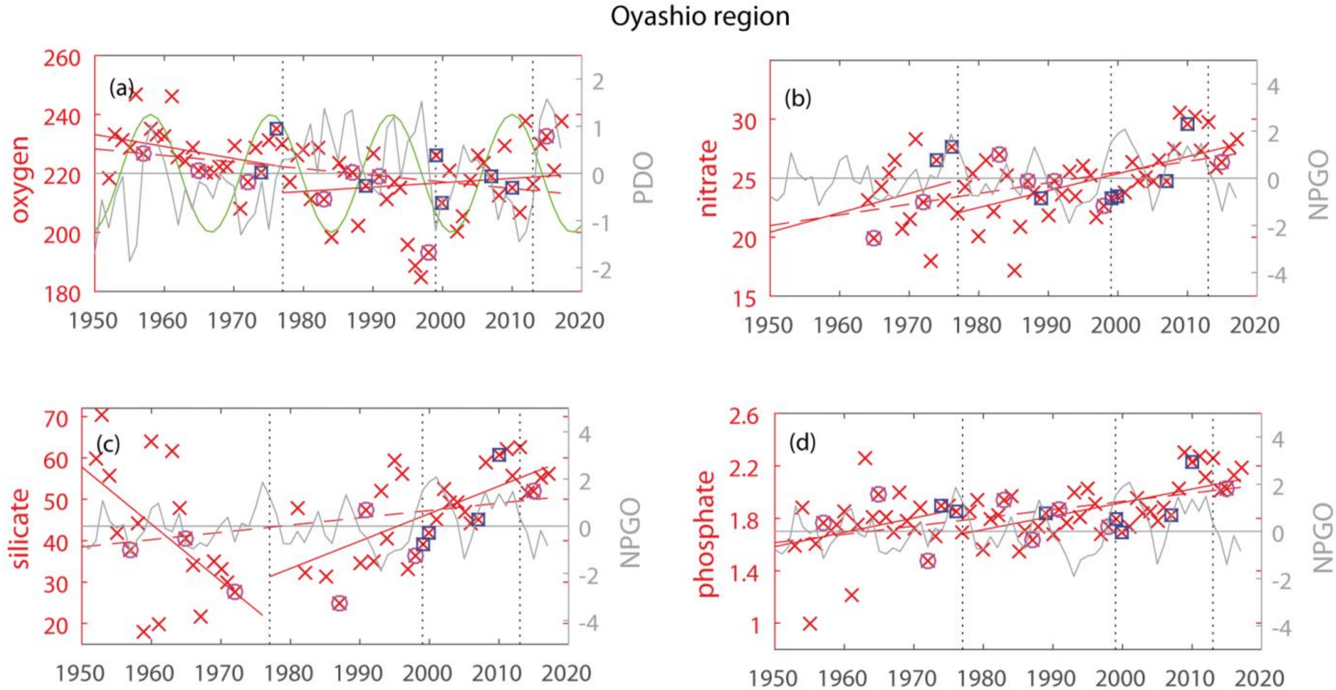

Figure 7. Annual mean concentration (in μmol kg^{-1}, red crosses) for years available and trends for the layer 50 to 300 m plotted for the periods 1950 to 1976 for the negative PDO phase and after 1976 for the positive PDO phase (solid red lines) and for the entire time period (dashed red lines) for the Oyashio region (39° - 42°N, 144° - 149°E) from hydrodata CTD and bottle data and a data collection used in Whitney et al. (2013) and Sasano et al. (2018) in μmol kg^{-1} yr^{-1} for a) oxygen, b) nitrate, c) silicate and d) phosphate. For nitrate measurements in 1963 were removed as the 50-300 m mean was much too high (1.27 μmol kg^{-1}). El Niño years defined as strong are marked by an additional magenta circle, strong La Niña years by an additional blue square. The change of the PDO status in 1977, 1999 and 2013 are marked by vertical dotted lines. In the oxygen time series the 18.6 year sinusoidal nodal cycle is included (green curve). The annual mean PDO index is shown in the oxygen time series as grey curve and the annual mean NPGO index is shown in the nitrate, silicate and phosphate time series as grey curve.

Supplementary table

Table S1. Linear trends of solutes in µmol kg^{-1} yr^{-1} with 95% confidence intervals where data are available for the entire period since 1950, for negative (1950-1976; PDO-) and positive (after 1976; PDO+) PDO periods in the 50 to 300 m depth layer for April to December measurements for area P (48°-52°N, 143°-147°W) and Oyashio region (39°-42°N, 144°-149°E). Trends whose 95% confidence interval includes zero are shown in *italics*.

Parameter	trend	time period	PDO- trend	time period	PDO+ trend	time period
Area	area P		area P		area P	
Oxygen	*-0.22± 0.23*	1954-2017	*-0.16 ± 1.44*	1954-1976	*-0.22 ± 0.43*	1977-2017
Nitrate	+0.069 ± 0.050	1956-2017	*-0.114 ± 0.516*	1956-1973	+0.069 ± 0.050	1980-2017
Silicate	+0.491 ± 0.177	1958-2017	*+2.26 ± 5.74*	1958-1971	+0.216 ± 0.211	1987-2017
Phosphate	*+0.001 ± 0.003*	1954-2017	*-0.014 ± 0.025*	1954-1971	*+0.001 ± 0.007*	1980-2017
Area	Oyashio region		Oyashio region		Oyashio region	
Oxygen	*-0.18 ± 0.32*	1952-2017	*-0.27 ± 0.56*	1952-1976	*+0.14 ± 0.72*	1977-2017
Nitrate	+0.106 ± 0.043	1964-2017	*+0.365 ± 0.566*	1964-1976	+0.124 ± 0.060	1977-2017
Silicate	*+0.156 ± 0.340*	1952-2017	-1.40 ± 1.14	1952-1971	+0.614 ± 0.343	1981-2017
Phosphate	+0.006 ± 0.003	1953-2017	*+0.011 ± 0.017*	1953-1976	+0.009 ± 0.005	1977-2017

Supplementary figures

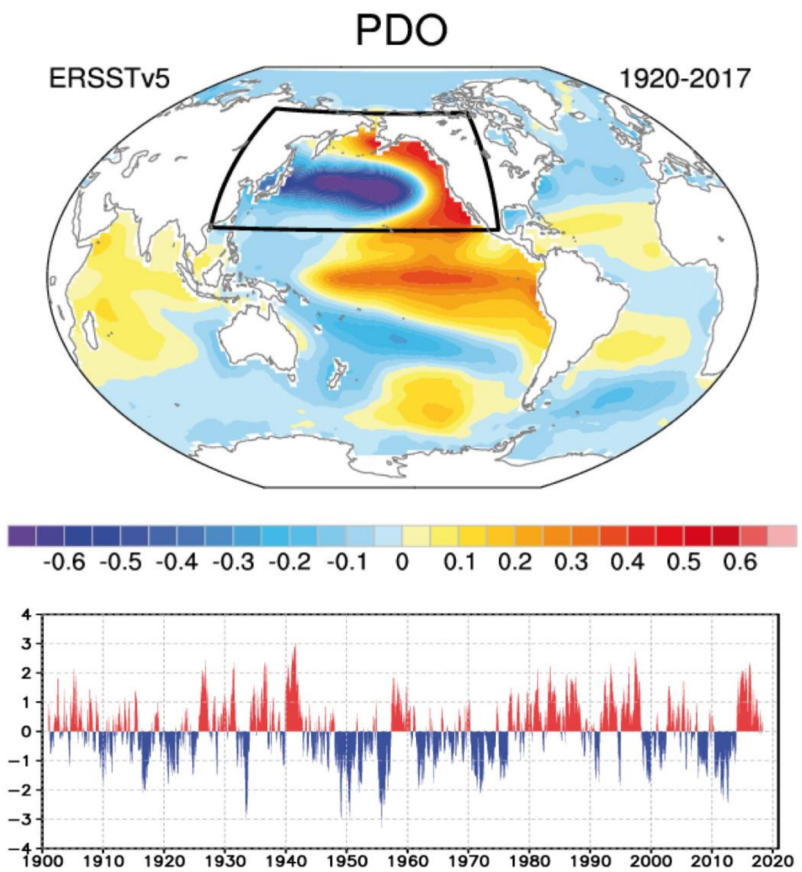

Figure S1. Global expression of the Pacific Decadal Oscillation (PDO, top) obtained by linearly regressing monthly sea surface temperature (SST) anomalies (in °C) based on ERSSTv5 data set (Huang et al., 2017) for the period 1920-2017 at each grid box upon the leading Principal Component (PC) time series based on the domain outlined in the black box (Adapted from Deser et al., 2010 and modified by A. Phillips). The PDO time series 1900 to 2017, defined by their corresponding PC is shows in the lower frame. (Figure from Tokyo Climate Center, http://ds.data.jma.go.jp/tcc/tcc/products/elnino/decadal/pdo_month.html) based on the HadlSST data set (Rayner et al., 2003).

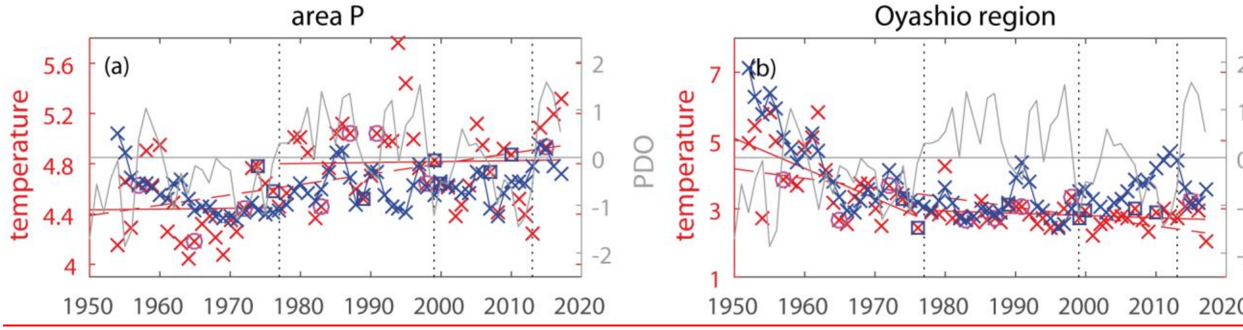

Figure S2. Annual mean concentration of temperature in °C for years available and trends for the layer 50 to 300 m plotted for the entire time period (dashed red lines) and for the periods 1950 to 1976 for the negative PDO phase and after 1976 for the positive PDO phase (solid red lines) a) at area P (48° to 52°N, 143° to 147°W) from hydrodata CTD and bottle data and station P data (50°N, 145°W) for the period 1954 to 2017 with a trend of 0.0083 +/- 0.0073 °C yr^{-1} and b) the Oyashio region between 39° and 42°N, 144° and 149°E for the period 1952 to 2017 with a trend of -0.0273+/-0.0188 °C yr^{-1}. El Niño years defined as strong are marked by an additional magenta circle, strong La Niña years by an additional blue square. The change of the PDO status in 1977, 1999 and 2013 are marked by vertical dotted lines. PDO annual time series are shown in the temperature time series as solid grey lines. In addition the annual mean 0 to 50 m temperatures smoothed with a 4-point running mean are included as blue lines covering the temperature range 6.0 to 10.2 °C in area P and 5.3 to 16.4°C in the Oyashio region.

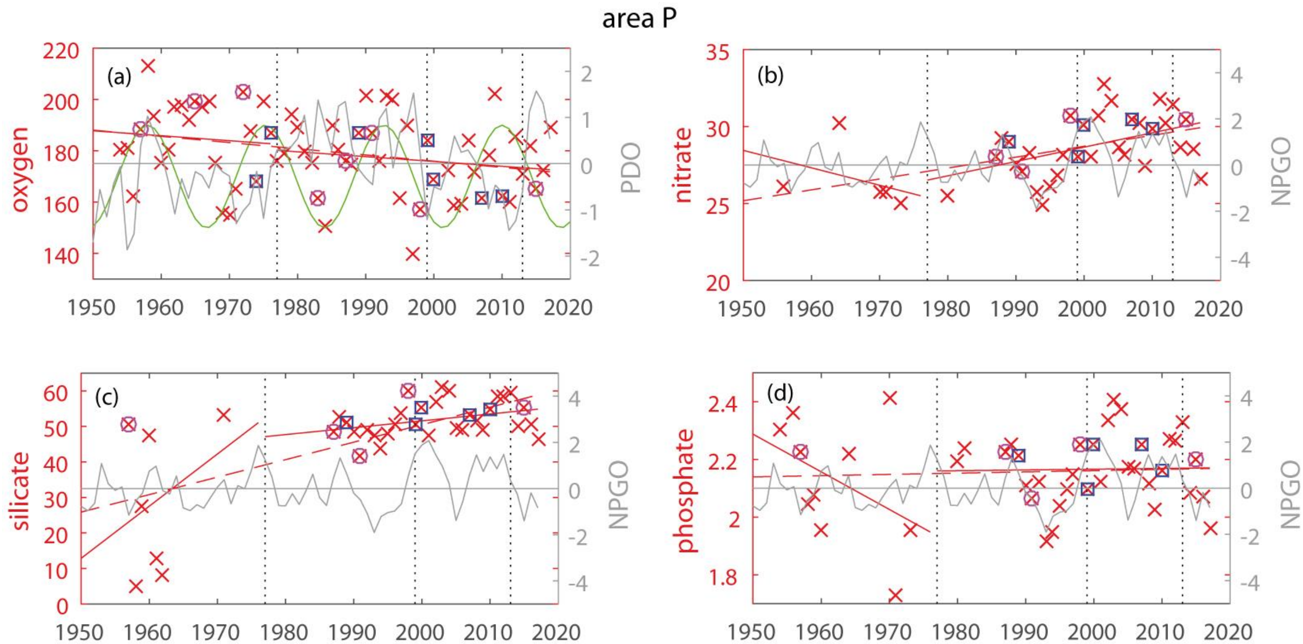

Figure S3. Annual mean concentration (in µmol kg^{-1}, red crosses) for years available and trends for the layer 50 to 300 m plotted for the entire time period (dashed red lines) and for the periods 1950 to 1976 for the negative PDO phase and after 1976 for the positive PDO phase (solid red lines) at area P (48° to 52°N, 143° to 147°W) from hydrodata CTD and bottle data and station P data (50°N, 145°W) for the period since 1956 in µmol kg^{-1} yr^{-1} for a) oxygen, b) nitrate, c) silicate and d) phosphate. For oxygen measurements in 2001 were removed as the 50-300 m mean was much to high (379 µmol kg^{-1}). El Niño years defined as strong are marked by an additional magenta circle, strong La Niña years by an additional blue square. The change of the PDO status in 1977, 1999 and 2013 are marked by vertical dotted lines. The PDO annual mean time series are shown in the oxygen time series and the NPGO annual mean time series in nitrate, phosphate and silicate time series as solid grey lines. In the oxygen time series the 18.6 year sinusoidal nodal cycle is included (green curve).

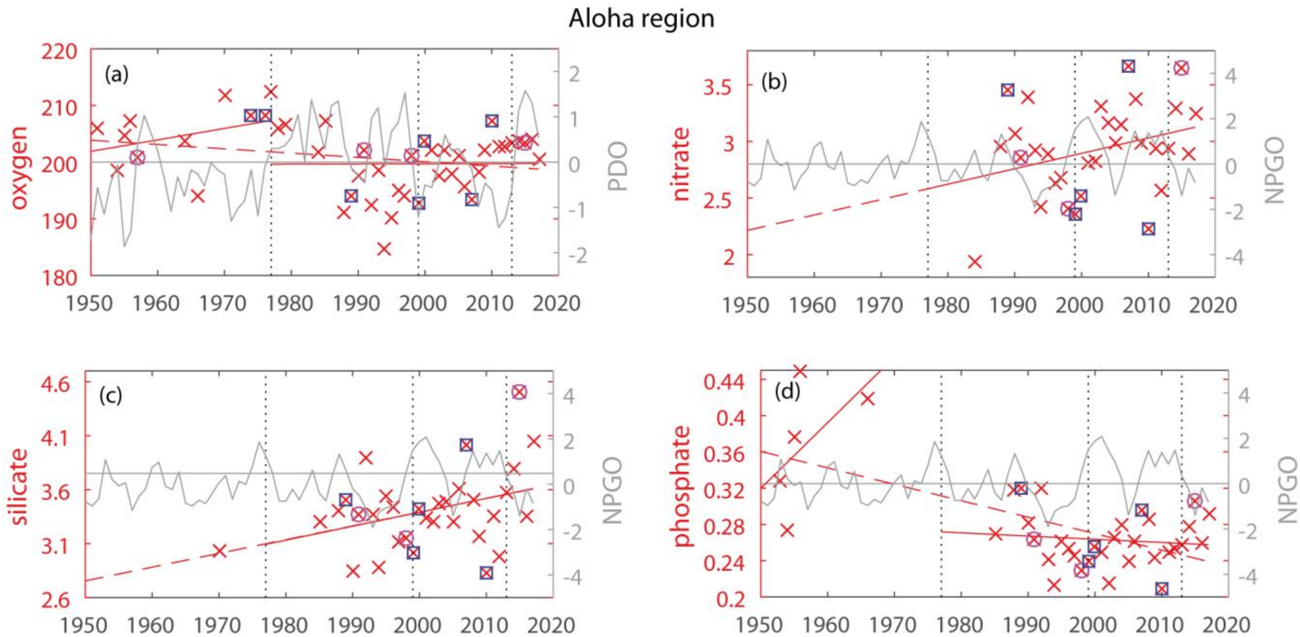

Figure S4. Annual mean concentration (in µmol kg^{-1}, red crosses) for years available and trends for the layer 50 to 300 m plotted for the entire time period (dashed red lines) and for the periods 1950 to 1976 for the negative PDO phase after 1976 for the positive PDO phase (solid red lines) between 22° and 25°N, 156 and 159°W from hydrodata CTD and bottle data and station Aloha data (22°45'N, 158°W) for the period since October 1988 in µmol kg^{-1} yr^{-1} for a) oxygen, b) nitrate, c) silicate and d) phosphate. For silicate measurements in 1984 were removed as they were to low (1.83 µmol kg^{-1}) phosphate measurements in 1951 were removed as the 50-300 m mean was to high (0.573 µmol kg^{-1}). El Niño years defined as strong are marked by an additional magenta circle, strong La Niña years by an additional blue square. The change of the PDO status in 1977, 1999 and 2013 are marked by vertical dotted lines. PDO annual mean time series are shown in the oxygen time series and the NPGO annual mean time series in nitrate, phosphate and silicate time series as solid grey lines.

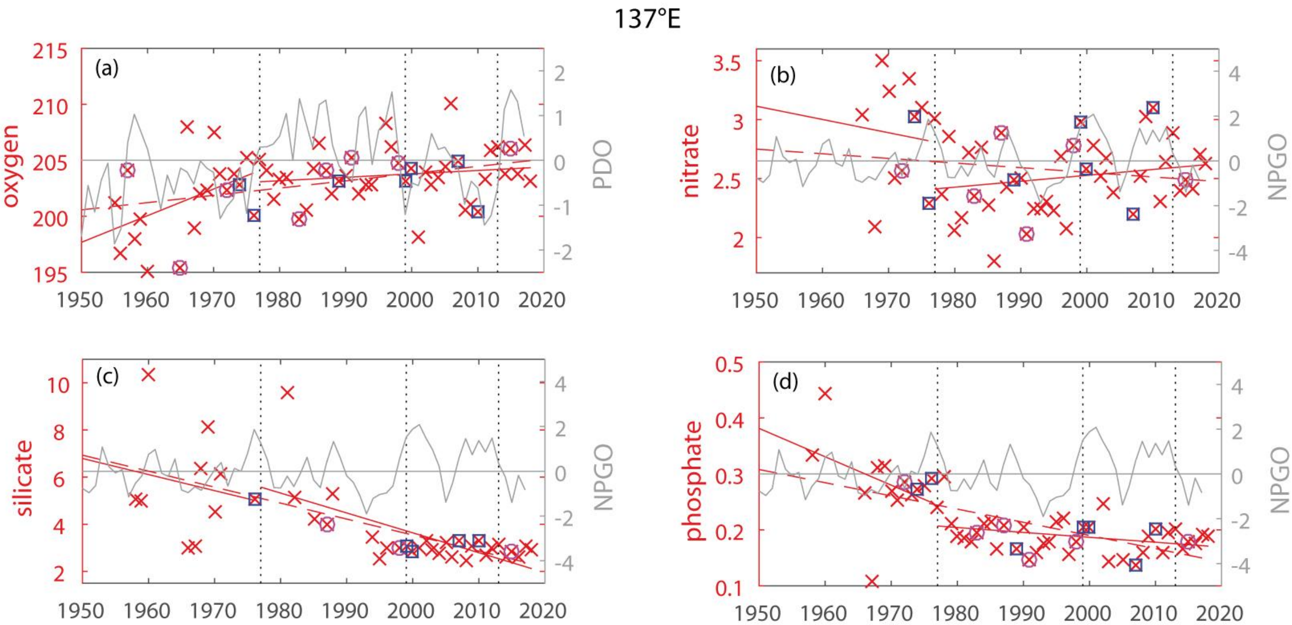

Figure S5. Annual mean concentration (in μmol kg^{-1}, red crosses) for years available and trends for the layer 50 to 300 m plotted for the entire time period (dashed red lines) and for the periods 1950 to 1976 for the negative PDO phase and after 1976 for the positive PDO phase (solid red lines) between 20° and 26°N, 134 and 140°E from hydrodata CTD and bottle data in μmol kg^{-1} yr^{-1} for a) oxygen, b) nitrate, c) silicate and d) phosphate. For oxygen measurements in 1982 and 1995 were removed as they were to high/low (1982: 236 μmol kg^{-1}, 1995: 185 μmol kg^{-1}), for nitrate 1959 was removed 14.4 μmol kg^{-1} and for silicate 1983 23.7 μmol kg^{-1}. El Niño years defined as strong are marked by an additional magenta circle, strong La Niña years by an additional blue square. The change of the PDO status in 1977, 1999 and 2013 are marked by vertical dotted lines. PDO annual mean time series are shown in the oxygen time series and the NPGO annual mean time series in the nitrate, silicate and phosphate time series as solid grey lines.

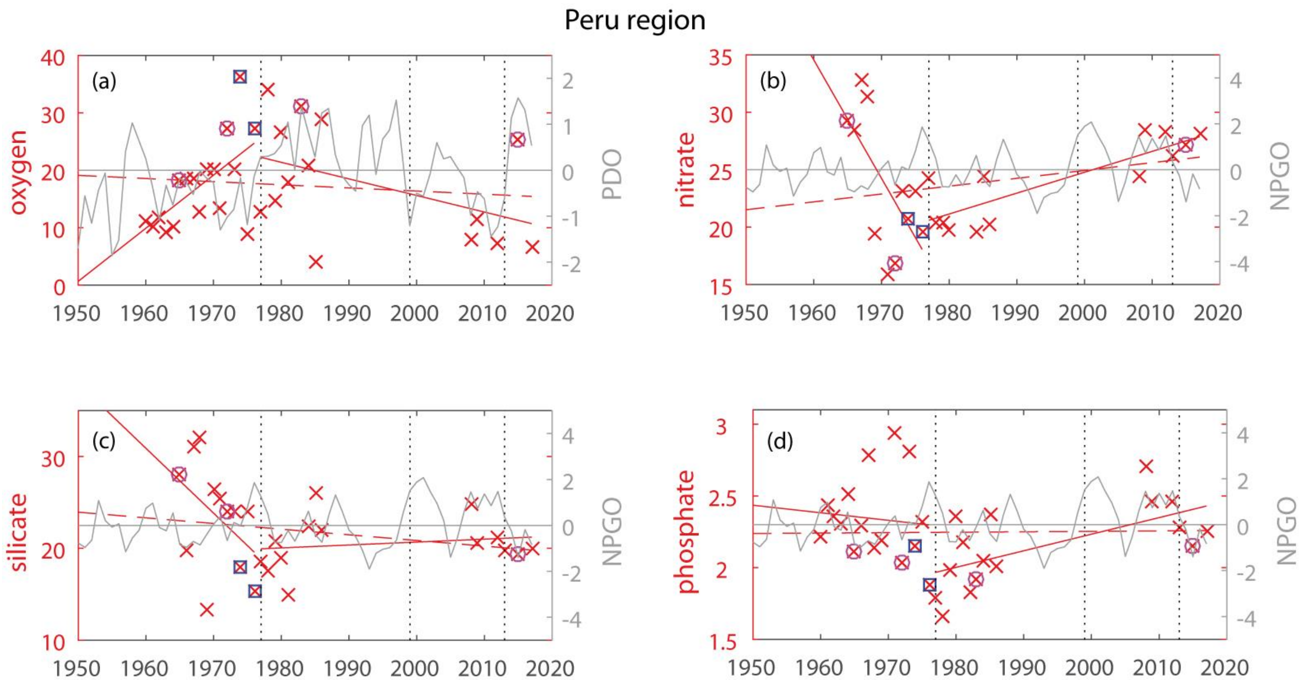

Figure S6~~5~~. Annual mean concentration (in µmol kg^{-1}, red crosses) for years available and trends for the layer 50 to 300 m plotted for the entire time period (dashed red lines) and for the periods 1950 to 1976 for the negative PDO phase and after 1976 for the positive PDO phase (solid red lines) between 7° and 12°S, 78 and 83°W from hydrodata CTD and bottle data in µmol kg^{-1} yr^{-1} for a) oxygen, b) nitrate, c) silicate and d) phosphate. For oxygen measurements in 1982 were removed as they were to high (62.4 µmol kg^{-1}). El Niño years defined as strong are marked by an additional magenta circle, strong La Niña years by an additional blue square. The change of the PDO status in 1977, 1999 and 2013 are marked by vertical dotted lines. PDO annual mean time series are shown in the oxygen time series and the NPGO annual mean time series in the nitrate, silicate and phosphate time series as solid grey lines.

Supplementary references:

Deser, C., Alexander, M. A., Xie, S.-P., and Phillips, A. S.: Sea surface temperature variability: Patterns and mechanisms, Annu. Rev. Mar. Sci., 2, https.//doi.org/10.1146/annurev-marine-120408-151453, 2010.

Huang, B., Thorne, P. W., Banzon, V. F., Boyer, T., Cherupin, G., Lawrimore, J. H., Menne, M. J., Smith, T. M., Vose, R. S., and Zhang, H.-M.: Extended reconstructed sea surface temperature, version 5 (ERSSTv5): Upgrades, validations, and intercomparisons, J. Climate, 30, https://doi.org/10.1175/JCLI-D-16-0836.1, 2017.

Rayner, N. A., Parker, D. E., Horton, E. B., Folland, C. K., Alexander, L. V., Rowell, D. P., Kent, E. C., and Kaplan, A.: Global analyses of sea surface temperature, sea ice, and night marine air temperature since the late nineteenth century, J. Geophys. Res. 108 D14, 4407, https://doi.org/10.1029/2002JD002670, 2003.